The emergence of successful *Streptococcus pyogenes* lineages through convergent pathways of capsule loss and recombination directing high toxin expression

Claire E. Turner[1,2#], Matthew T. G. Holden[3,4], Beth Blane[5], Carolyne Horner[6], Sharon J. Peacock[5], Shiranee Sriskandan[2].

[1]Molecular Biology & Biotechnology, The Florey Institute, University of Sheffield

[2]Department of Infectious Diseases, Imperial College London

[3]Pathogen Genomics, The Wellcome Trust Sanger Institute, Cambridge, United Kingdom

[4] School of Medicine, University of St Andrews, St Andrews, United Kingdom

[5] Department of Medicine, University of Cambridge, Cambridge, United Kingdom

[6] British Society for Antimicrobial Chemotherapy, Birmingham, United Kingdom

Corresponding author:

Dr Claire Turner

c.e.turner@sheffield.ac.uk

Running head: Convergent evolution in *Streptococcus pyogenes*

Abstract

Gene transfer and homologous recombination in *Streptococcus pyogenes* has the potential to trigger the emergence of pandemic lineages, as exemplified by lineages of *emm*1 and *emm*89 that emerged in the 1980s and 2000s respectively. Although near-identical replacement gene transfer events in the *nga* (NADase) and *slo* (Streptolysin O) loci conferring high expression of these toxins underpinned the success of these lineages, extension to other *emm*-genotype lineages is unreported. The emergent *emm*89 lineage was characterised by five regions of homologous recombination additional to *nga/slo*, including complete loss of the hyaluronic acid capsule synthesis locus *hasABC,* a genetic trait replicated in two other leading *emm* types and recapitulated by other *emm* types by inactivating mutations. We hypothesised that other leading genotypes may have undergone similar recombination events. We analysed a longitudinal dataset of genomes from 344 clinical invasive disease isolates representative of locations across England, dating from 2001 to 2011, and an international collection of *S. pyogenes* genomes representing 54 different genotypes, and found frequent evidence of recombination events at the *nga-slo* locus predicted to confer higher toxin expression. We identified multiple associations between recombination at this locus and inactivating mutations within *hasA/B,* suggesting convergent evolutionary pathways in successful genotypes. This included common genotypes *emm*28 and *emm*87. The combination of no or low capsule, and high expression of *nga* and *slo,* may underpin the success of many emergent *S. pyogenes* lineages of different genotypes, triggering new pandemics and could change the way *S. pyogenes* causes disease.

Importance

Streptococcus pyogenes is a genetically diverse pathogen, with over 200 different genotypes defined by *emm* typing, but only a minority of these genotypes are responsible for the majority of human infection in high income countries. Two prevalent genotypes associated with disease rose to international dominance following recombination of a toxin locus that conferred increased expression. Here, we found that recombination of this locus and promoter has occurred in other diverse genotypes, events that may allow these genotypes to expand in the population. We identified an association between the loss of hyaluronic acid capsule synthesis and high toxin expression, which we propose may be associated with an adaptive advantage. As *S. pyogenes* pathogenesis depends both on capsule and toxin production, new variants with altered expression may result in abrupt changes in the molecular epidemiology of this pathogen in the human population over time.

Introduction

The capacity for the bacterial human pathogen *Streptococcus pyogenes* to undergo genetic exchange, independent of known bacteriophages or mobile elements, is not well understood, yet recent evidence suggests it underpins the emergence of successful new variants that rapidly rise to international dominance. Homologous recombination of a chromosomal region encompassing the toxin genes *nga* (encoding for NADase), *ifs* (encoding the inhibitor for NADase) and *slo* (encoding for Streptolysin O), which was dated to have occurred in the mid-1980s, is thought to have driven the rise of *emm*1 to almost global dominance (1). The homologous recombination event resulted in increased *nga*/*slo* expression compared to the previous variant, linked to the gain of a highly active *nga-ifs-slo* promoter in the new *emm*1 variant compared to the previous variant (2).

A very similar recombination event was recently identified in the genotype *emm*89. A new variant of *emm*89 sequence type (ST) 101 (also referred to as Clade 3) emerged, having undergone six regions of predicted homologous recombination compared to its ST101 predecessor (also referred to as Clade 2) (3, 4). One of the six regions encompassed the *nga-ifs-slo* locus, comprising a region almost identical to *emm*1, that conferred similarly high expression of *nga* and *slo* compared to the previous variant. Another recombination region within the emergent ST101 *emm*89 resulted in the loss of the hyaluronic acid capsule. We dated the emergence of this new acapsular, high toxin expressing ST101 *emm*89 lineage to the mid-1990s, but there was a rapid increase and rise to dominance in the UK between 2005-2010 (3). The lineage is now the dominant form of *emm*89 in the UK as well as other parts of the world including Europe, North America and Japan (4-8).

Given that recombination associated with *nga-ifs-slo* can give rise to new successful *S. pyogenes* variants, we hypothesised that this may be a feature common to other successful

emm-types. To determine if this is the case, we sequenced the genomes of 344 *S. pyogenes* invasive disease isolates originating from hospitals across England between 2001-2011, and compared the data with other available historical and contemporary international *S. pyogenes* whole genome sequence (WGS) data. We identified that recombination of the *nga-ifs-slo* locus has occurred in other leading *emm*-types, supporting the hypothesis that it can underpin the emergence and success of new lineages. We also identified an association of *nga-ifs-slo* recombination towards a high activity promoter variant with inactivating mutations within the capsule locus. This suggests that loss of capsule may also provide an advantage to certain genotypes, either through a direct effect on pathogenesis or an association with the process of recombination.

Results

Genetic characterisation of bacteraemia isolates

We performed whole genome sequencing of 344 *S. pyogenes* invasive isolates collected from hospitals across England by the British Society for Antimicrobial Chemotherapy (BSAC) Bacteraemia Resistance Surveillance Programme during 2001-2011. Forty-four different *emm*-types were identified from *de novo* assembly, with the most common being *emm*1 (n=64, 18.6%), *emm*12 (n=34, 9.9%), *emm*89 (n=32, 9.3%), *emm*3 (n=28, 8.1%), *emm*87 (n= 22, 6.4%) and *emm*28 (n=15, 4.4%) (Figure S1). Antimicrobial susceptibilities were typical for *S. pyogenes* with 100% isolates susceptible to penicillin, and 22% resistant to clindamycin, erythromycin and/or tetracycline; detailed susceptibilities and associated genotypes are reported in Dataset S1.

The phylogenetic distribution of the 344 isolates based on core genome variation revealed distinct clustering by *emm*-type, each forming single lineages with the exceptions of *emm*44,

*emm*90 and *emm*101, each of which formed two lineages (Figure 1A). Pairwise distances between isolates gave a median of just 45 SNPs separating the genomes of isolates of the same *emm*-genotype (range 0-15,137 SNPs), compared to a median of 15,648 SNPs separating the genomes of isolates of different *emm*-types (range 5,312-18,317 SNPs) (Figure 1B). The genotypes *emm*44, *emm*90 and *emm*101 gave the highest SNP distance for the intra-*emm* comparison (13,494 - 15,137 SNPs) which approaches the median level observed between *emm*-types. This indicated that while other genotypes represent a relatively conserved chromosomal genetic background, the populations of *emm*44, *emm*90 and *emm*101 exhibit more diverse chromosomal backgrounds despite representing the same *emm*-type, potentially due to *emm* gene switching.

High level of variation within the nga-ifs-slo *locus*

In order to identify the level of variation within the *nga-ifs-slo* locus we extracted the sequence from the 3' end of *nusG* (immediately upstream of *nga*) to the 3' end of *slo* (P-*nga-ifs-slo*), comprising the entire locus and all upstream sequence including the predicted ~67bp *nga/ifs/slo* promoter region (9). We constructed a phylogenetic tree from SNPs within the P-*nga-ifs-slo* region from the genomes of isolates belonging to the most common *emm*-types and compared it to the phylogeny constructed with SNPs extracted from a whole genome comparison to a reference *emm*89 genome, H293 (Figure 2). Most *emm* genotypes were associated with a single P-*nga-ifs-slo* variant that was unique to that genotype. The main exception to this was the P-*nga-ifs-slo* variant found in modern (post 1980s M1T1) *emm*1, as this was also found in all *emm*12, all *emm*22 (a lineage known to be acapsular), and 11 of the 32 *emm*89 isolates. These 11 *emm*89 represented the emergent acapsular ST101 variant, whilst the remaining 21 *emm*89 isolates represented the original encapsulated ST101 variant, with a different unique P-*nga-ifs-slo* as previously reported (3). The entire *emm*75 population and one of the two *emm*76 isolates were also associated with a P-*nga-ifs-slo* variant that was

closely related to the *emm*1-like variant. All but two *emm*87 isolates had a P-*nga-ifs-slo* variant also found in the acapsular lineage *emm*4. The presence of multiple P-*nga-ifs-slo* variants within the *emm*76 and *emm*87 genotypes, where the core chromosome was otherwise relatively conserved, indicated that gene transfer and recombination are responsible for the P-*nga-ifs-slo* variation in these genotypes rather than extensive genome-wide divergence or *emm* 'switching'.

Variants of the nga-ifs-slo *promoter associated with altered expression*

Recombination of P-*nga-ifs-slo* and surrounding regions in *emm*1 and *emm*89 conferred higher activity and expression of NGA (NADase) and SLO (1, 3, 10). This change in expression was linked to the combination of three key residues at -27, -22 and -18 within the *nga-ifs-slo* promoter. $A_{-27}G_{-22}T_{-18}$ at these key sites was associated with high *nga-ifs-slo* promoter activity in *emm*1 and emergent *emm*89 following recombination (also referred to as Pnga3) compared to low promoter activity of historical *emm*1 and *emm*89, associated with the key site combinations $A_{-27}T_{-22}C_{-18}$ and $G_{-27}T_{-22}T_{-18}$ respectively (2) (Figure 3A). We compared the ~67bp *nga-ifs-slo* promoter region of the 344 BSAC collection isolate genomes to identify different variants. We expanded the data analysed by including assembled genome data from over 5000 isolates representing 54 different *emm* types: from Cambridge University Hospital (CUH) (12), the rest of England and Wales collected by Public Health England (PHE) in 2014/2015 (PHE-2014/15) (13, 14) and from the USA collected by the Active Bacterial Core Surveillance System (ABCs) in 2015 (ABCs-2015) (15). We excluded 39 *emm*-types represented by fewer than 3 isolates (Dataset S2).

Four combinations of the -27, -22 and -18 residues were found across all 5271 isolates (Table 1); variant 1 $A_{-27}T_{-22}C_{-18}$ and variant 2 $G_{-27}T_{-22}T_{-18}$ are associated with low promoter activity, while variant 3 $A_{-27}G_{-22}T_{-18}$ and variant 4 $A_{-27}T_{-22}T_{-18}$ are associated with high promoter

activity. We also identified subtypes of the 67bp promoter region which varied at bases other than -27, -22 and -18 (Figure 3A and B, Table 1). $A_{-27}T_{-22}C_{-18}$ variant subtype 1.1 and $G_{-27}T_{-22}T_{-18}$ variant subtype 2.1 have both previously been confirmed to have low promoter activity (2) and were the most common variants found across genotypes. Other subtypes of these variants were restricted to single genotypes except $G_{-27}T_{-22}T_{-18}$ variant subtype 2.2, which differed by a single substitution of C for a T residue at -40bp. Two subtypes of the high activity variant $A_{-27}G_{-22}T_{-18}$ were found, the most common being subtype 3.1 associated with *emm*1 and emergent *emm*89, and subtype 3.2 which was found predominantly in the genomes of *emm*4 and *emm*87, and differed from subtype 3.1 by a single substitution of G for T at -40bp. We measured the activity of NADase in the culture supernatant of strains representing different promoter subtypes and found that the presence of T/G/C at -40bp did not affect activity of the promoter (Figure S2). The fourth promoter variant, $A_{-27}T_{-22}T_{-18}$ is also associated with high activity (11) and was identified in the genomes of *emm*28, *emm*75 and all *emm*78. Only three *emm*-types were exclusively associated with the high activity promoter variant $A_{-27}G_{-22}T_{-18}$; *emm*1, *emm*3 and *emm*12. Other *emm*-types with the high activity promoter variant also had one or more of the other three promoter variants, suggesting a mixed population or, as in the case of *emm*89, an evolving population.

We sought evidence for acquisition of the high activity-associated promoter $A_{-27}G_{-22}T_{-18}$ variant by *emm* genotypes where the dominant or ancestral state was a low activity-associated promoter; these included, in addition to the aforementioned *emm*89: *emm*75, *emm*76, *emm*77, *emm*81, *emm*82, *emm*87, *emm*94 and *emm*108, all of which are *emm* types frequently identified in the UK and the USA (13-15). Although one *emm*28 was found to carry the high activity-associated $A_{-27}G_{-22}T_{-18}$ promoter, the rest of the *emm*28 population was divided between either $A_{-27}T_{-22}C_{-18}$ or $A_{-27}T_{-22}T_{-18}$ variants. The data pointed to a switch in P-*nga*-*ifs*-

176 *slo* in all cases rather than an *emm* switch, except for *emm*82, where the *emm*82 gene has
177 replaced the *emm*12 gene in an *emm*12 genetic background (15).

178 *High level of mutations within the capsule locus leading to truncations of HasA or HasB*

179 As well as recombination around the P-*nga-ifs-slo* region, the emergent ST101 variant of
180 *emm*89 had also undergone recombination surrounding the *hasABC* locus, and, in place of the
181 *hasABC* genes, was a region of 156bp that was not found in genotypes with the capsule locus
182 but is found in the acapsular *emm*4 and *emm*22 isolates (3). To identify any similar events in
183 other genotypes, we examined the sequences of *hasA*, *hasB*, and *hasC* in the assemblies of
184 isolates from the BSAC collection as well as CUH (12), PHE-2014/15 (13,14) and ABCs-
185 2015 (15) collections for gene presence as well as premature stop codon mutations or missing
186 genes (Figure 4). The *hasABC* locus was absent in the majority of *emm*89 isolates, consistent
187 with the previous observations describing the recent emergence of the acapsular *emm*89
188 variant (3). Similarly, the *hasABC* genes were absent in all *emm*4 and *emm*22 isolates, as
189 previously identified (16), except for two *emm*4 isolates and one *emm*22 isolate which had an
190 intact *hasABC* locus predicted to encode full length proteins. We confirmed the genotypes of
191 these isolates by *emm*-typing the assembled genomes; MLST and phylogenetic analysis
192 indicated they both had a very different genetic background to other *emm*4 or *emm*22
193 populations suggesting these were not typical of these *emm* types, and therefore they
194 represent examples of *emm* switching. Interestingly, we also identified a similar replacement
195 of *hasABC* for the 156bp region in one *emm*28 isolate (PHE-2014/15, GASEMM1261 (14)),
196 but phylogenetic analysis suggested this was highly divergent to the rest of the *emm*28
197 population, likely to represent another example of *emm* switching. Isolated examples of
198 individual *hasA* or *hasB* gene loss were identified in the genomes of isolates belonging to
199 *emm*1 (n=1), *emm*3 (n=1), *emm*11 (n=1), *emm*12 (n=4) and *emm*108 (n=2).

The majority of genotypes (n=35/54, 65%) had isolates without genes or truncation mutations in at least one of *hasABC* genes (Figure 4). Mutations in *hasC* were rare and only detected in one isolate, an *emm*77 which also had a mutation within *hasA*. Within seven of the eight *emm*-types for which we identified potential P-*nga-ifs-slo* recombination, a high percentage of isolates had inactivating mutations in *hasA* and *hasB* suggesting a possible association between an acapsular genotype/phenotype and recombination of P-*nga-ifs-slo* to gain a high activity promoter. Including the previously identified *emm*1 and *emm*89 recombination events, P-*nga-ifs-slo* recombination to gain a high activity promoter was detected in 10 genotypes and in all 10 genotypes (100%) were isolates with *hasA/B* gene mutations or gene absence. However, in the 44 genotypes that had not undergone P-*nga-ifs-slo* recombination to gain a high activity promoter, significantly fewer (25/44, 57%) had isolates with *hasA/B* gene mutation or gene absence ($\chi^2_{1df} = 6.662$, p=0.0098).

*Recombination of P-*nga-ifs-slo *and surrounding regions*

To confirm our prediction that genotypes *emm*28, *emm*75, *emm*76, *emm*77, *emm*81, *emm*87, *emm*94 and *emm*108 had undergone recombination around P-*nga-ifs-slo*, we mapped all the genome sequence data for each genotype to the *emm*89 reference genome H293. Gubbins analysis of SNP clustering predicted regions of recombination spanning the *nga-ifs-slo* region and varying in length in all eight genotypes (Figure 5). To analyse recombination of these genotypes and potential capsule loss further, we studied the population structure of each genotype individually.

Recombination within emm*28 and* emm*87 around P-*nga-ifs-slo *and the capsule locus*

The genotypes *emm*28 and *emm*87 were the sixth and fifth most common in the BSAC collection, and *emm*28 has previously been noted to be a major cause of infection in high

income countries (17). We focussed attention on *emm*28 and *emm*87 as there has been little genomic work on these genotypes so far.

All BSAC *emm*28 isolates carried the $A_{-27}T_{-22}C_{-18}$ low activity associated promoter but inclusion of international genomic data identified $A_{-27}T_{-22}T_{-18}$ variant carrying isolates. These two promoter variants were associated with different major lineages within the entire population of 379 international *emm*28 isolates, including one newly sequenced English isolate originally isolated in 1938. The majority of isolates (n=373) clustered either with the reference MGAS6180 strain (USA) (18) or with the reference MEW123 strain (USA) (19) (Figure 6A). Gubbins analysis for core SNP clustering predicted that the two lineages were distinguished by a single 28,200bp region of recombination, between positions 142,426bp (*ntpE*, M28_Spy0126) and 170,625bp (M28_Spy0153) of the MGAS6180 chromosome. This suggests the emergence of one lineage from the other through a single recombination event, followed by expansion of both lineages (Figure 6B). Within the recombination region was the P-*nga*-*ifs*-*slo* locus, which differed between the two lineages; although unique in the MGAS6180-like lineage and with low activity associated promoter residues $A_{-27}T_{-22}C_{-18}$, the MEW123-like lineage had a P-*nga*-*ifs*-*slo* identical to that found in *emm*78 isolates, with the three key residues of $A_{-27}T_{-22}T_{-18}$. This is supported by recent findings identifying two main lineages within *emm*28 and that the $A_{-27}T_{-22}T_{-18}$ promoter variant conferred greater toxin expression than $A_{-27}T_{-22}C_{-18}$ (11).

Although we identified an $A_{-27}G_{-22}T_{-18}$ high activity variant of P-*nga*-*ifs*-*slo* within *emm*28, this was only associated with the highly divergent GASEMM1261 isolate that may represent an *emm* switching event. This isolate, along with three other PHE-2014/15 isolates (GASEMM2648, GASEMM1396 and GASEMM1353) also representing highly divergent lineages, were excluded from the phylogenetic analysis.

All *emm*28 isolates, regardless of lineage and including MGAS6180 (originally isolated in the 1990s), had the same insertion mutation within *hasA* of an A residue after 219 bp. This insertion was predicted to lead to a frameshift and a premature stop codon after 72 amino acids (aa) instead of full length 420 aa, rendering *hasA* a pseudogene. Some isolates also had additional mutations in *hasA*; a deletion of an A residue in a septa-A tract leading to a frameshift and a stop codon after 7 aa (n=1); a deletion of a T residue in a septa-T tract leading to a frameshift and a stop codon after 15 aa (n=2); an insertion of an A residue after 57 bp leading to a frameshift and a stop codon after 46 aa (n=3). The loss of full length HasA would render the isolates acapsular.

In *emm*28 there were just two exceptions where *hasA* found to be intact: the historical *emm*28 isolate from 1938 had an intact *hasABC* capsule operon; and BSAC_bs2099, which appeared to have undergone recombination to acquire a 22,316bp region surrounding the *hasABC* genes, that was 99% identical to the same region in *emm*2 isolate MGAS10270, suggesting *emm*2 might be the donor for this recombination. Both isolates were predicted to express full length HasA and synthesise capsule. Taken together, in comparison with the oldest *emm*28 isolate, the data showed that post 1930s *emm*28 isolates became acapsular through mutation, but the contemporary population is divided into two major lineages, MEW123-like and MGAS6180-like lineages, that may differ in *nga-ifs-slo* expression. Additionally, there was evidence of geographical structure in the population: the MEW123-like lineage comprised mainly of North American isolates (39/44) and only five from England/Wales; isolates from Australia, France and Lebanon were MGAS6180-like, along with the rest of the England/Wales isolates.

Phylogenetic analysis of the BSAC *emm*87 population was expanded and compared with publicly available *emm*87 genome sequence data, totalling 173 isolate genomes from the UK and North America, including one historical NCTC UK isolate from ~1970-80 (NCTC12065,

Genbank accession number GCA_900460075.1). Gubbins analysis predicted a single 20,506bp region of recombination surrounding the P-*nga-ifs-slo* region, that distinguished the main population from the oldest BSAC isolates from 2001 and the historical 1970-80 NCTC isolate (Figure 6C). Whilst the two 2001 BSAC isolates and the NCTC isolate had a P-*nga-ifs-slo* variant with low activity-associated promoter residues, $G_{27}T_{-22}T_{-18}$, all other *emm*87 isolates had a P-*nga-ifs-slo* region with high activity associated promoter residues, $A_{-27}G_{-22}T_{-18}$, identical to that found in *emm*4 and some *emm*77. This suggested the emergence of a new lineage through a single recombination event followed by expansion within the population, redolent of that previously observed in *emm*89 (Figure 6D).

Similar to *emm*28, all *emm*87 isolates, bar four had an insertion of an A residue after 57 bp that resulted in a frameshift mutation in *hasA*, and the introduction of a premature stop codon after 46aa of HasA. This mutation was also identified within the historical NCTC isolate but was not found in the two 2001 BSAC isolates, that had an intact *hasABC* locus. This mutation was also absent in two PHE-2014/15 isolates that had undergone an additional recombination event (32,243bp) surrounding the *hasABC* locus, although, as this region shared 100% DNA identity to *emm*28 isolate MGAS6180, HasA is truncated. Overall the data showed that, like *emm*89, contemporary *emm*87 are acapsular with a high activity *nga-ifs-slo* promoter, suggesting that this *emm* lineage may have recently shifted towards this genotype/phenotype.

Recombination within different multi-locus sequence types of emm*75*

The *emm*75 genotype is of interest as a common cause of non-invasive infection in the UK; it is also used in models of nasopharyngeal infection (28, 29). Eleven *emm*75 isolates were present in the BSAC collection, all multilocus sequence type (ST) 150. When we incorporated other available genome sequence data for *emm*75 (n=174), including two newly sequenced historical English *emm*75 isolates from 1937 and 1938, two major lineages were

identified, characterised by two different MLSTs; ST49 or ST150 (Figure 7A). Although the two historic English isolates were ST49, like the majority of modern North American isolates, the modern England/Wales isolates were predominantly ST150.

Although these two ST lineages differed in the P-*nga-ifs-slo* region there was a high level of predicted recombination across the genomes of both STs, perhaps indicative of historic *emm* switching or extensive genetic exchange. ST49 isolates had the subtype 1.1 low activity $A_{-27}T_{-22}C_{-18}$ promoter, whereas all ST150 isolates had the $A_{-27}G_{-22}T_{-18}$ subtype 3.1 high activity promoter variant, identical to that of *emm*1/*emm*89. Modern ST49 isolates did, however, differ from historic 1930s isolates by ten distinct regions of predicted recombination (Figure 7B), including a region spanning the *nga-ifs-slo* locus, although this did not include the promoter region. We did not detect any mutations affecting the capsule region in *emm*75. Taken together, *emm*75 was characterised by two major MLST lineages differing in P-*nga/ifs/slo* promoter activity genotypes but without evidence of recent recombination or loss of capsule.

Lineages associated with recombination in emm*76,* emm*77 and* emm*81.*

The phylogeny of all available genome data for *emm*76, *emm*77 and *emm*81 confirmed the presence of diverse lineages, associated with different MLSTs (Figure 8A-C). In all genotypes, however, there was a dominant MLST lineage representing the majority of isolates; ST50 *emm*76, ST63 *emm*77 and ST624 *emm*81. Within the dominant MLST lineages of *emm*76 and *emm*77, there were sub-lineages that were associated with different P-*nga-ifs-slo* variants as well as loss of functional HasA through mutation.

We identified five different MLSTs within *emm*76 (Figure 8A), but the majority of isolates (30/38) belonged to ST50, including both BSAC isolates. Recombination analysis of the ST50 lineage identified a sub-lineage that differed from other ST50 isolates by 19 regions of

recombination (Figure S3). One of these regions encompassed P-*nga-ifs-slo*, conferring a P-*nga-ifs-slo* variant closely related to that of modern *emm*1 and *emm*89 with an identical high activity promoter (subtype 3.1). This sub-lineage was dominated by PHE-2014/15 isolates and also contained the more recent of the two BSAC isolates (2008). All isolates in this sub-lineage, except one, also had a nonsense mutation within *hasA* of a C to T change at 646bp, resulting in a premature stop codon after 215aa, likely to render the isolates acapsular. Only one ST50 isolate outside this sub-lineage had the same *hasA* C646T change. All other *emm*76 isolates would express full length HasA.

Two sub-lineages were also identified within the dominant *emm*77 lineage ST63 (Figure 8B), and one was associated with the high activity cluster P-*nga-ifs-slo* variant, compared to predicted low activity variants found in the other *emm*77 lineages. Recombination analysis predicted only two regions of recombination distinguishing the two sub-lineages; a region of 17,954bp surrounding P-*nga-ifs-slo*, and a 173bp region within a hypothetical gene (SPYH293_00394) (Figure S4). Whilst all BSAC *emm*77 isolates (years 2001-2009) were ST63 with low activity P-*nga-ifs-slo*, PHE isolates from 2014-2015 were almost evenly divided between the two sub-lineages, indicating a potential recent change in England/Wales. All ST63 isolates except two, had a deletion of a T residue within a septa-polyT tract at 458bp in *hasA*, predicted to truncate the HasA protein after 154aa. The two exceptions were predicted to encode full length HasA and were associated with low P-*nga-ifs-slo* promoter activity variants. Although also not associated with high P-*nga-ifs-slo* promoter activity variants, other lineages of *emm*77 also carried mutations within *hasA* that would truncate HasA; ST399 isolates carried an insertion of a T residue at 71 bp of the *hasA* gene resulting in a premature stop codon after 46 aa, and two ST133 isolates carried G894A substitution resulting in a premature stop codon after amino acid residue 297.

The *emm*81 population (n=68) was more diverse with nine different sequence types (Figure 8C), but the majority of isolates (41/68) were ST624 or the single locus variant ST837 (9/68; one SNP in *recP* allele) within the same lineage. ST171 was restricted to three historical isolates originally collected in 1938-1939. We did not detect any *hasABC* variations that would disrupt translation in *emm*81 lineages except for the dominant group of ST624/ST837, where we identified an A residue insertion at 128 bp in *hasB* resulting in a frameshift and premature stop codon after 50 aa. All ST624/ST837 carried the high activity cluster P-*nga-ifs-slo* variant identical to that seen in *emm*3, compared to all other lineages associated with other low activity P-*nga-ifs-slo* variants. Recombination analysis identified extensive recombination had occurred within *emm*81 leading to the different levels of diversity, but we identified one region of recombination that distinguished the ST624/ST837 lineage from the closely related ST909 and ST117 populations (Figure S5). This region surrounded the P-*nga-ifs-slo* locus, suggesting ST624/ST837 gained the high activity cluster P- *nga-ifs-slo* variant through recombination, like other *emm*-types, potentially from *emm*3. The emergence of the high activity P-*nga-ifs-slo* variant and truncated HasB ST624/ST837 lineage may be recent in England/Wales as all BSAC isolates obtained prior to 2009 were outside of this lineage.

High activity cluster P-nga-ifs-slo *variants gained by recombination in* emm*94 and* emm*108*

Within *emm*94, we identified a P-*nga-ifs-slo* identical to that found in *emm*1 with high activity promoter variant subtype 3.1. Phylogenetic analysis of 51 *emm*94 isolates identified a dominant lineage among England/Wales isolates separate to the single USA isolate and two England/Wales isolates (Figure S6A), that belonged to ST89. Gubbins analysis predicted 11 regions of recombination in all lineage associated isolates compared to the three outlying isolates, including one (22,648bp) that encompassed P-*nga-ifs-slo*, transferring a high activity $A_{-27}G_{-22}T_{-18}$ P-*nga-ifs-slo* variant. All *emm*94 isolates contained an indel within *hasB*

compared to the reference (H293); losing 6bp and gaining 13bp between 127-133bp. This variation causes a frameshift and would truncate the HasB protein after 45aa.

We identified a similar high activity cluster P- *nga-ifs-slo* variant within a single *emm*108 genome originating from the USA. Within the 9 isolates from PHE-2014/15 (n=7) and ABCs-2015 (n=2), there were two sequence types, ST1088 and ST14. ST14 was represented by the only two ABCs-2015 isolates and we identified that both had lost the entire *hasB* gene, although *hasA* and *hasC* were still present (Figure S6B). Additionally, one of the ABCs-2015 isolates had undergone recombination of a single ~29,683bp region surrounding the P-*nga-ifs-slo,* replacing P-*nga-ifs-slo* for one identical to that found in *emm*3 with high activity promoter variant $A_{-27}G_{-22}T_{-18}$ subtype 3.1.

Mobile genetic elements and antimicrobial resistance

The acquisition of mobile genetic elements such as prophages and transposons may also be influenced by capsule expression and can also influence the expansion and success of new lineages. We therefore determined the presence of prophage-associated superantigen and DNase genes as well as antimicrobial resistance genes to estimate the number of mobile genetic elements present within each isolate of the genotypes *emm*28, *emm*75, 76, 77, 81, 87, 94 and 108 (Figures S3-S5, Dataset S3). On average there were 4.4 elements present in isolates predicted to express full length HasABC, compared to 2.5 elements present in isolates with *hasABC* gene mutations or gene absence, suggesting that the presence of capsule does not hinder mobile genetic elements. We also detected no link between lineages within these genotypes that had undergone P-*nga-ifs-slo* recombination and mobile factors, except within *emm*76 and *emm*77. Isolates belonging to the *emm*76 ST50 sub-lineage associated with HasA mutation and P-*nga-ifs-slo* recombination, all carried the prophage-associate superantigen genes *speH* and *speI* as well as a diverse variant of the DNAse *spd3* and the

erythromycin resistance gene *ermB* (Figure S3). This differed to the other ST50 isolates that carried another variant of *spd3* and multiple different resistance genes. The sub-lineage of ST63 *emm*77 associated with P-*nga-ifs-slo* recombination also carried *spd3* and all, except one isolate, carried the erythromycin resistance gene *ermTR*; both genes were not common in other ST63 *emm*77 isolates (Figure S4).

Discussion

The emergence of new, internationally successful lineages of *S. pyogenes* can be driven by recombination-related genome remodelling, as demonstrated by *emm*1 and *emm*89. The transfer of a P-*nga-ifs-slo* region conferring increased expression to the new variant was common to both genotypes. In the case of *emm*89, five other regions of recombination were identified in the emergent variant, one resulting in the loss of the hyaluronic acid capsule. Although potentially all six regions of recombination combined underpinned the success of the emergent *emm*89, we have shown here that recombination of P-*nga-ifs-slo* has occurred in other leading *emm*-types as well as a high frequency of capsule loss through mutation. These data point to an association between genetic change affecting capsule and recombination affecting the P-*nga-ifs-slo* locus, conferring increased production of *nga-ifs-slo*; in some cases, (notably *emm*87, *emm*89, and *emm*94) this has further been associated with an apparent fitness advantage and expansion within the population.

A number of genotypes were found to be associated with multiple variants of P-*nga-ifs-slo*. The majority of genotypes had P-*nga-ifs-slo* variants with the low activity promoter associated three key residues variants: $G_{-27}T_{-22}T_{-18}$ or $A_{-27}T_{-22}C_{-18}$. Only *emm*1, *emm*3 and *emm*12 were exclusively associated with the high activity $A_{-27}G_{-22}T_{-18}$ variant. We have shown that the same high activity promoter variant is present in isolates belonging to twelve other *emm* types, notably, *emm*76, *emm*77, *emm*81, *emm*87 and *emm*94, although this is not a

consistent feature in these genotypes due to *emm*-switching or recombination. We identified four combination of the three key promoter residues and several subtypes of the 67bp promoter that varied in bases other than those at the -27, -22, and -18 key positions. Although some subtypes were restricted to single genotypes, variation in the -40 base led to the subtype 2.2 of $G_{-27}T_{-22}T_{-18}$ and subtype 3.2 of $A_{-27}G_{-22}T_{-18}$. We measured the activity of NADase in representative strains and genotypes of these promoter variants and found that variation in the -40 base did not impact on the activity conferred by the -27, -22, and -18 bases. Although we predicted the level of *nga* and *slo* expression based on the promoter variant, this may not relate to actual expression given the level of other genetic variation between genotypes. However, our consistent findings of lineages emerging following acquisition of the high activity promoter variant supports the hypothesis that this confers some benefit that may relate to increased toxin expression.

Intriguingly, where we identified an acquisition of the high activity promoter variant through recombination, these genotypes also had a genetic change in the capsule locus, likely rendering the organism unable to make capsule (*hasA* mutation) or only low levels of capsule (*hasB* mutation). To date, only *emm*4, *emm*22, and the emergent *emm*89 lineage are known to lack all three genes required to synthesise capsule. Here, we identified mutations that would truncate HasA and HasB in 35% of all isolates and 65% (35/54) of all genotypes. As the majority of isolates included in this study were invasive or sterile site isolates, the findings further challenge the dogma that the hyaluronan capsule is required for full virulence of *S. pyogenes* and, in addition, lend credence to the possibility that the increased expression of NADase and SLO may in some way compensate for the lack of capsule (31). While capsule has been shown to underpin resistance to opsonophagocytic killing in the most constitutively hyper-encapsulated genotypes such as *emm*18 (32, 33), there is less evidence that it contributes measurably to opsonophagocytosis killing resistance in other genotypes (3).

Whether loss of capsule synthesis is of benefit to *S. pyogenes* is uncertain; the capsule may shield several key adhesins used for interaction with host epithelium and fomites, but may also act as a barrier to transformation with DNA. An accumulation of *hasABC* inactivating mutations have been identified during long term carriage (34) and, although for some genotypes capsule loss impacted on survival in whole human blood, a high number of acapsular *hasA* mutants have also recently been found to be causing a high level of disease in children, including *emm*1, *emm*3 and *emm*12 (35).

The process of recombination in *S. pyogenes* is not well understood and natural competence has only been demonstrated once and under conditions of biofilm or nasopharyngeal infection (36). We do not know if the six regions of recombination that led to the emergence of the new ST101 *emm*89 variant occurred simultaneously, although no intermediate isolates have been identified. The loss of the hyaluronic acid capsule in the new emergent *emm*89, along with our consistent findings of inactivating mutations associated with P-*nga-ifs-slo* transfer indicate either 1) the process of recombination requires the inactivation of capsule, 2) capsule negative *S. pyogenes* requires high expression of *nga-ifs-slo* for survival, 3) or that a capsule negative phenotype combined with high expression of *nga-ifs-slo* provides a greater selective advantage to *S. pyogenes*.

The phylogeny of *emm*28, *emm*87, *emm*77, *emm*94, and *emm*108 indicated that mutations in *hasA* or *hasB* occurred prior to recombination of P-*nga-ifs-slo*, supporting the first hypothesis that prior capsule inactivation is required for recombination. There is no evidence, however, to suggest this was required for recombination in the *emm*1 population. It could be hypothesised that capsule acts as a barrier to genetic exchange, but there has also been a positive genetic association of capsule to recombination rates (37). A positive association may, however, be related only to species expressing antigenic capsule whereby recombination is required to introduce variation for immune escape.

The *hasC* gene is not essential for capsule synthesis (38) because a paralog of *hasC* exists within the *S. pyogenes* genome. A paralog for *hasB* (*hasB.2*) also exists elsewhere in the *S. pyogenes* chromosome and can act in the absence of *hasB* to produce low levels capsule (39) but *hasA* is absolutely essential for capsule synthesis (38). The mutations in *hasA* in *emm*28 and *emm*87 have been previously noted and confirmed to render the isolates acapsular (35, 40). Not all acapsular isolates were found to carry the high activity promoter of *nga-ifs-slo*, despite being invasive, perhaps refuting the hypothesis that high activity *nga-ifs-slo* promoter is essential for the survival of acapsular *S. pyogenes*. High expression of *nga-ifs-slo* may also occur through other mechanisms, for example through mutation in regulatory systems. We looked at the sequences of *covR/S* and *rocA*, known to negatively regulate *nga-ifs-slo*, in all isolates (Dataset S2) and identified some *emm*-type specific variants, consistent with our previous findings (12). We did not identify any other genotypes where all isolates carried truncation mutations in *rocA*, like *emm*3 and *emm*18 that have been previously confirmed to affect function and increase expression of *rocA/covR* regulated virulence factors (32, 41), consistent with other findings (15). It is unclear as to whether the amino acid changes in found in other genotypes would affect function of *rocA* as well as *covR* and *covS* and this requires further work.

Interestingly, we identified that the capsule locus is also a target for recombination as, like *emm*89, isolates within *emm*28 and *emm*87 had undergone recombination of this locus and surrounding regions, varying in length and restoring capsule synthesis in *emm*28. Isolated examples of *hasA* or *hasB* gene loss were identified in some genotypes, such as *emm*108, possibly due to internal recombination and deletion.

Only two *emm*4 and one *emm*22 isolates were found to have P-*nga-ifs-slo* variants that were not $A_{-27}T_{-22}G_{-18}$ high activity promoter variants, and interestingly these isolates carried the *hasABC* genes, typically absent in *emm*4 and *emm*22. The high genetic distance of these

isolates to other *emm*4 and *emm*22 genomes indicated potential *emm* switching of the *emm*4 or *emm*22 genes onto different genetic backgrounds. The single *emm*28 with a high activity P-*nga*-*ifs*-*slo* variant may also be an example of this, and was one of four *emm*28 isolates that did not cluster with the two main *emm*28 lineages. Although we excluded them from our analysis as we focussed on recombination within the two main lineages, the presence of highly diverse variants within genotypes and the potential for *emm*-switching warrants further investigation, particularly as the most promising current vaccine is multi-valent towards common M-types (42).

All other genotypes carrying the high activity P-*nga*-*ifs*-*slo* variant were found to have undergone recombination of this region; *emm*28, *emm*75, *emm*76, *emm*77, *emm*81, *emm*87, *emm*94 and *emm*108, as well as the previously described *emm*1 and *emm*89.

Within *emm*87, we identified three isolates outside of the main population lineage that represented the oldest isolates in the collection; two from 2001 (different geographical locations within England) and one NCTC strain from ~1970-80 (NCTC12065). A single region of recombination, surrounding the P-*nga*-*ifs*-*slo* locus distinguished the main population lineage from the three older isolates, consistent with a recombination event but, due to a lack of earlier isolates of *emm*87, we could not confirm a recombination related shift in the population, as reported previously for *emm*89 and *emm*1.

The existence of two lineages within the contemporary *emm*28 suggests that one has not yet displaced the other, although the MEW123-like lineage was predominantly USA isolates, consistent with recent findings (11). The P-*nga*-*ifs*-*slo* region with the high activity associated $A_{-27}T_{-22}T_{-18}$ and acquired through recombination by the MEW123-like lineage was identical to that found in *emm*78, indicating *emm*78 as the potential genetic donor. We found *emm*78 to have high levels of NADase activity, as predicted, and interestingly, like *emm*28, all eight

*emm*78 isolates were acapsular due to a deletion within the *hasABC* promoter region extending into *hasA*. This again may support the hypothesis that capsule negative *S. pyogenes* require high expression of *nga-ifs-slo* for survival.

A strength of this study was the systematic longitudinal sampling over a 10 year period; as expected, this again identified the shift in the *emm*89 population. Other *emm*-types exhibited lineages with different P-*nga-ifs-slo* variants, and those with the more active promoter variant did appear to become dominant over time, similar to *emm*1 and the emergent *emm*89 lineages. For example, the high activity P-*nga-ifs-slo* ST63 lineage of *emm*77 was not detected in England/Wales isolates prior to 2014-15. Similarly, the high activity P-*nga-ifs-slo* variant *emm*81 ST646/ST837 lineage was represented by only a single isolate (of six) collected 2001-2009 but became dominant by 2014/15 in England/Wales and the USA. *emm*75 was the 6th most common genotype in England/Wales 2014-15 and dominated by high activity P-*nga-ifs-slo* variant ST150 lineage, yet less common in the USA where ST49 with low activity P-*nga-ifs-slo* is dominant. A high prevalence of *emm*94 was also found in England/Wales 2014-15 but was rare in the USA (only 1 isolate). Our analysis of this genotype indicated there has been a recombination related change in the population as we detected 11 regions of predicted recombination including P-*nga-ifs-slo* potentially conferring high toxin expression. The other ten regions of recombination may also provide advantages to this lineage along with a potential low level of capsule through *hasB* mutation.

Other factors may also contribute to the success of emergent new lineages, including mobile prophage associated virulence factors and antimicrobial resistance genes. Acquisition of mobile genetic elements did not appear to be affected by capsule loss, indeed fewer mobile genetic element associated factors were detected in isolates with capsule gene mutations than in isolates with functional capsule genes. A number of bacteriophages that target *S. pyogenes* encode a hyaluronidase thought to allow the bacteriophage to access the bacterial surface by

degrading the outer capsule layer (43), therefore recombination of these elements is likely to be different to gene transfer of core genetic regions, like P-*nga-ifs-slo*.

We did, however, identify an association in the lineages of *emm*76 and *emm*77 with prophage-associated virulence factors and antimicrobial resistance genes. It is possible that the superantigens *speH*, *speI* and DNAse *spd3* may also contribute to the success of the lineages that had undergone P-*nga-ifs-slo* recombination. Of concern is that both *emm*76 and *emm*77 carried genes for resistance to tetracycline and erythromycin which were rarer in other genotypes. If the acapsular/high-toxin expressing lineages do expand in the population, it will be important to monitor the levels of antimicrobial resistance in these lineages. This is also true for *emm*108, as *tetM* was detected in all isolates, but the presence of antimicrobial resistance genes was rare in *emm*28, *emm*75, *emm*81, *emm*87 and *emm*94, regardless of lineage.

The development and boosting of circulating antibodies to SLO is often used as a diagnostic biomarker of recent *S. pyogenes* infection and is known to be more specific to throat rather than skin infections. The genomic analysis provides explanation for this historic and well-recognized association between anti- SLO titres and disease patterns, due to known tissue tropism of *S. pyogenes emm* types. Whether the alteration of SLO activity in different *S. pyogenes* strains might render such a test more or less specific will be of interest, although may explain observed differences in ASO titre between genotypes (44). There is also the possibility that other beta haemolytic streptococci might acquire similarly active SLO production, reducing the specificity of ASO titre to *S. pyogenes*.

Our genomic analysis has uncovered convergent evolutionary pathways towards capsule loss and recombination related re-modelling of the P-*nga-ifs-slo* locus in leading contemporary genotypes. This suggests that a combination of capsule loss and gain of high *nga-ifs-slo*

expression provides a greater selective advantage than either of these phenotypes alone. Acquisition of the high activity promoter led to pandemic *emm*1 and *emm*89 clones that are dominant and highly successful. Active surveillance of the lineages comprising *emm*76, *emm*77, *emm*81, *emm*87, *emm*94 and *emm*108 is required to determine if capsule loss/reduction and recombination of P-*nga*-*ifs*-*slo* towards high expression will trigger expansion towards additional pandemic clones in the next few years.

Materials & Methods

Isolates

344 isolates of *S. pyogenes* associated with blood stream infections and submitted to the British Society for Antimicrobial Chemotherapy (BSAC, www.bsacsurv.org) from 11 different sites across England between 2001-2011 were subjected to whole genome sequencing (Dataset S1). All BSAC isolates were tested for antibiotic susceptibility using the BSAC agar dilution method to determine MICs (45).

A further six isolates were sequenced from a historical collection of *S. pyogenes* originally collected in the 1930s from puerperal sepsis patients at Queen Charlottes Hospital, London, UK; one *emm*28 from 1938 (ERR485803), two *emm*75 from 1937 (ERR485807) and 1939 (ERR485820), three *emm*81 from 1938 (ERR485805) and 1939 (ERR485801, ERR485802).

Genome sequencing

Streptococcal DNA was extracted using the QIAxtractor instrument according to the manufacturer's instructions (QIAgen, Hilden, Germany), or manually using a phenol-chloroform method (46). DNA library preparation was conducted according to the Illumina protocol and sequencing was performed on an Illumina HiSeq 2000 with 100-cycle paired-end runs. Sequence data have been submitted to the European Nucleotide Archive (ENA) (www.ebi.ac.uk/ena) (accession numbers in Datasets S1 and S2).

588 Genomes were *de novo* assembled using Velvet with the pipeline and improvements found
589 at https://github.com/sanger-pathogens/vr-codebase and https://github.com/sanger-
590 pathogens/assembly_improvement (47). Annotation was performed using Prokka. *emm*
591 genotypes were determined from the assemblies and multilocus sequence types (MLSTs)
592 were identified using the MLST database (pubmlst.org/spyogenes) and an in-house script
593 (https://github.com/sanger-pathogens/mlst_check). New MLST were submitted to the
594 database (https://pubmlst.org/).

595 **Genome sequence analysis**

596 Sequence reads were mapped using SMALT (https://www.sanger.ac.uk/science/tools/smalt)
597 to the completed *emm*89 reference genome H293 (HG316453.2) (3) as this genome contains
598 no known prophage regions. Other reference genomes were also used where indicated with
599 predicted prophage regions (Table S1) excluded to obtain 'core' SNPs. Maximum-likelihood
600 phylogenetic trees were generated from aligned core SNPs using RAxML (48) with the GTR
601 substitution model and 100 bootstraps. Regions of recombination were predicted using
602 Gubbins analysis using the default parameters (49). Branches of phylogenetic trees were
603 coloured according to bootstrap support using iTOL (50).

604 Other genome sequence data were obtained from the short read archive. We combined data
605 collected across England and Wales through Public Health England during 2014 and 2015
606 (PHE-2014/15) supplied by Kapatai *et al*. (14) and Chalker *et al*. (13) from invasive and non-
607 invasive *S. pyogenes* isolates. We also used data supplied by Chochua et al. (15) collected by
608 Active Bacterial Core Surveillance USA in 2015 (ABCs-2015) from invasive *S. pyogenes*
609 isolates. ABCs-2015 sequence data was pre-processed by Trimmomatic (51) to remove
610 adapters and low quality sequences. PHE-2014/15 had already been pre-processed (13, 14).
611 Genome data from these collections were assembled *de novo* using Velvet (assembly

statistics provided in Dataset S2) and any isolates with greater than 2.2Mbp total assembled length and/or more than 500 contig numbers were excluded. We also used data from Turner *et al*. (2017) of invasive and non-invasive isolates from the Cambridgeshire region, UK and collected through Cambridge University Hospital (CUH) (12). We relied on the *emm*-type determined during the original studies and excluded any data where the *emm*-type was uncertain or negative. The genes *hasA, hasB, hasC, covR, covS, rocA* and the P-*nga*-*ifs*-*slo* were extracted from the assembled genome using *in silico* PCR (https://github.com/simonrharris/in_silico_pcr). Capsule locus and P-*nga*-*ifs*-*slo* variants were also confirmed through manual inspection of mapping data where genotype could not be accurately determined from assembly.

Mapping of *emm*76, *emm*77 and *emm*81 sequence data was performed using *de novo* assembled genome data from one BSAC collection isolate representing the equivalent genotype. Prophage regions were predicted using PHASTER (52) and removed before SNP extraction.

Antimicrobial resistance genes were identified by srst2 (53) using the ARG-ANNOT database (ARGannot_r2.fasta) (54). The presence of prophage associated superantigen genes *speA, speC, speH, speI, speL, speL, speM* and *ssa* were determined using srst2 and the feature database previously used by Chochua *et al*. (15) available at https://github.com/BenJamesMetcalf. The presence of prophage-associated DNAses genes *sda, sdn, spd1, spd3, spd3v6, spd4* was also determined using srst2 by adding regions of these genes to the feature database. Representative alleles of these DNAse genes were taken from previous analysis (55) to identify regions that would detect all variants of each DNAse, except we included *spd3v6* separate to *spd3* as it represents a divergent allele to *spd3*. Sequences used are available at Mendeley (DOI; 10.17632/hzwjkj2gtp.2).

NADase activity

Activity of NADase was measured in culture supernatant as previously described (3). Activity was determined as the highest dilution capable of hydrolysing NAD+. Isolates were selected from the BSAC collection to represent different promoter variants, and for which there were three or more isolates available and were lacking mutations in regulatory genes.

Conflict of interest

SJP is a consultant to Specific and Next Gen Diagnostics.

Acknowledgments

This publication presents independent research supported by the Health Innovation Challenge Fund (WT098600, HICF-T5-342), a parallel funding partnership between the Department of Health and Wellcome Trust. The work was also funded by the UK Clinical Research Collaboration (UKCRC, National centre for Infection Prevention & Management) and the National Institute for Health Research Biomedical Research Centre awarded to Imperial College London. The views expressed in this publication are those of the author(s) and not necessarily those of the Department of Health, NIHR, or Wellcome Trust. CET was an Imperial College Junior Research Fellow and is a Royal Society & Wellcome Trust Sir Henry Dale Fellow (208765/Z/17/Z).

References

1. **Nasser W, Beres SB, Olsen RJ, Dean MA, Rice KA, Long SW, Kristinsson KG, Gottfredsson M, Vuopio J, Raisanen K, Caugant DA, Steinbakk M, Low DE, McGeer A, Darenberg J, Henriques-Normark B, Van Beneden CA, Hoffmann S, Musser JM.** 2014. Evolutionary pathway to increased virulence and epidemic group A *Streptococcus* disease derived from 3,615 genome sequences. *Proc Natl Acad Sci U S A* **111:**E1768-1776.
2. **Zhu L, Olsen RJ, Nasser W, Beres SB, Vuopio J, Kristinsson KG, Gottfredsson M, Porter AR, DeLeo FR, Musser JM.** 2015. A molecular trigger for intercontinental epidemics of group A *Streptococcus*. *J Clin Invest* **125:**3545-3559.
3. **Turner CE, Abbott J, Lamagni T, Holden MT, David S, Jones MD, Game L, Efstratiou A, Sriskandan S.** 2015. Emergence of a new highly successful acapsular group A *Streptococcus* clade of genotype *emm*89 in the United Kingdom. *MBio* **6:**e00622.
4. **Zhu L, Olsen RJ, Nasser W, de la Riva Morales I, Musser JM.** 2015. Trading capsule for increased cytotoxin production: contribution to virulence of a newly emerged clade of *emm*89 *Streptococcus pyogenes*. *MBio* **6:**e01378-01315.
5. **Beres SB, Olsen RJ, Ojeda Saavedra M, Ure R, Reynolds A, Lindsay DSJ, Smith AJ, Musser JM.** 2017. Genome sequence analysis of *emm*89 *Streptococcus pyogenes* strains causing infections in Scotland, 2010-2016. *J Med Microbiol* **66:**1765-1773.
6. **Friaes A, Machado MP, Pato C, Carrico J, Melo-Cristino J, Ramirez M.** 2015. Emergence of the same successful clade among distinct populations of *emm*89 *Streptococcus pyogenes* in multiple geographic regions. *MBio* **6:**e01780-01715.
7. **Latronico F, Nasser W, Puhakainen K, Ollgren J, Hyyrylainen HL, Beres SB, Lyytikainen O, Jalava J, Musser JM, Vuopio J.** 2016. Genomic characteristics

behind the spread of bacteremic group A *Streptococcus* Type *emm*89 in Finland, 2004-2014. *J Infect Dis* **214:**1987-1995.

8. **Hasegawa T, Hata N, Matsui H, Isaka M, Tatsuno I.** 2017. Characterisation of clinically isolated *Streptococcus pyogenes* from balanoposthitis patients, with special emphasis on *emm*89 isolates. *J Med Microbiol* **66:**511-516.

9. **Kimoto H, Fujii Y, Yokota Y, Taketo A.** 2005. Molecular characterization of NADase-streptolysin O operon of hemolytic streptococci. *Biochim Biophys Acta* **1681:**134-149.

10. **Sumby P, Porcella SF, Madrigal AG, Barbian KD, Virtaneva K, Ricklefs SM, Sturdevant DE, Graham MR, Vuopio-Varkila J, Hoe NP, Musser JM.** 2005. Evolutionary origin and emergence of a highly successful clone of serotype M1 group A *Streptococcus* involved multiple horizontal gene transfer events. *J Infect Dis* **192:**771-782.

11. **Kachroo P, Eraso JM, Beres SB, Olsen RJ, Zhu L, Nasser W, Bernard PE, Cantu CC, Saavedra MO, Arredondo MJ, Strope B, Do H, Kumaraswami M, Vuopio J, Grondahl-Yli-Hannuksela K, Kristinsson KG, Gottfredsson M, Pesonen M, Pensar J, Davenport ER, Clark AG, Corander J, Caugant DA, Gaini S, Magnussen MD, Kubiak SL, Nguyen HAT, Long SW, Porter AR, DeLeo FR, Musser JM.** 2019. Integrated analysis of population genomics, transcriptomics and virulence provides novel insights into *Streptococcus pyogenes* pathogenesis. *Nat Genet* **51:**548-559.

12. **Turner CE, Bedford L, Brown NM, Judge K, Torok ME, Parkhill J, Peacock SJ.** 2017. Community outbreaks of group A *Streptococcus* revealed by genome sequencing. *Sci Rep* **7:**8554.

13. **Chalker V, Jironkin A, Coelho J, Al-Shahib A, Platt S, Kapatai G, Daniel R, Dhami C, Laranjeira M, Chambers T, Guy R, Lamagni T, Harrison T, Chand M, Johnson AP, Underwood A, Scarlet Fever Incident Management T.** 2017. Genome analysis following a national increase in Scarlet Fever in England 2014. *BMC Genomics* **18:**224.

14. **Kapatai G, Coelho J, Platt S, Chalker VJ.** 2017. Whole genome sequencing of group A *Streptococcus*: development and evaluation of an automated pipeline for emmgene typing. *PeerJ* **5:**e3226.

15. **Chochua S, Metcalf BJ, Li Z, Rivers J, Mathis S, Jackson D, Gertz RE, Jr., Srinivasan V, Lynfield R, Van Beneden C, McGee L, Beall B.** 2017. Population and whole genome sequence based characterization of invasive group A streptococci recovered in the United States during 2015. *MBio* **8**.

16. **Flores AR, Jewell BE, Fittipaldi N, Beres SB, Musser JM.** 2012. Human disease isolates of serotype m4 and m22 group A *Streptococcus* lack genes required for hyaluronic acid capsule biosynthesis. *MBio* **3:**e00413-00412.

17. **Steer AC, Law I, Matatolu L, Beall BW, Carapetis JR.** 2009. Global *emm* type distribution of group A streptococci: systematic review and implications for vaccine development. *Lancet Infect Dis* **9:**611-616.

18. **Green NM, Zhang S, Porcella SF, Nagiec MJ, Barbian KD, Beres SB, LeFebvre RB, Musser JM.** 2005. Genome sequence of a serotype M28 strain of group A *Streptococcus*: potential new insights into puerperal sepsis and bacterial disease specificity. *J Infect Dis* **192:**760-770.

729 19. **Jacob KM, Spilker T, LiPuma JJ, Dawid SR, Watson ME, Jr.** 2016. Complete
730 genome sequence of *emm*28 type *Streptococcus pyogenes* MEW123, a Streptomycin-
731 Resistant derivative of a clinical throat isolate suitable for investigation of pathogenesis.
732 *Genome Announc* **4**.
733 20. **Athey TB, Teatero S, Li A, Marchand-Austin A, Beall BW, Fittipaldi N.** 2014.
734 Deriving group A *Streptococcus* typing information from short-read whole-genome
735 sequencing data. *J Clin Microbiol* **52:**1871-1876.
736 21. **Long SW, Kachroo P, Musser JM, Olsen RJ.** 2017. Whole-Genome sequencing of a
737 human clinical isolate of *emm*28 *Streptococcus pyogenes* causing necrotizing fasciitis
738 acquired contemporaneously with Hurricane Harvey. *Genome Announc* **5**.
739 22. **Ibrahim J, Eisen JA, Jospin G, Coil DA, Khazen G, Tokajian S.** 2016. Genome
740 analysis of *Streptococcus pyogenes* associated with pharyngitis and skin infections.
741 *PLoS One* **11:**e0168177.
742 23. **Ben Zakour NL, Venturini C, Beatson SA, Walker MJ.** 2012. Analysis of a
743 *Streptococcus pyogenes* puerperal sepsis cluster by use of whole-genome sequencing.
744 *J Clin Microbiol* **50:**2224-2228.
745 24. **de Andrade Barboza S, Meygret A, Vincent P, Moullec S, Soriano N, Lagente V,**
746 **Minet J, Kayal S, Faili A.** 2015. Complete Genome Sequence of Noninvasive
747 *Streptococcus pyogenes* M/*emm*28 Strain STAB10015, Isolated from a Child with
748 Perianal Dermatitis in French Brittany. *Genome Announc* **3**.
749 25. **Longo M, De Jode M, Plainvert C, Weckel A, Hua A, Chateau A, Glaser P, Poyart**
750 **C, Fouet A.** 2015. Complete Genome Sequence of *Streptococcus pyogenes emm*28
751 Clinical Isolate M28PF1, Responsible for a Puerperal Fever. *Genome Announc* **3**.
752 26. **Athey TB, Teatero S, Sieswerda LE, Gubbay JB, Marchand-Austin A, Li A,**
753 **Wasserscheid J, Dewar K, McGeer A, Williams D, Fittipaldi N.** 2016. High

754 Incidence of Invasive Group A *Streptococcus* Disease Caused by Strains of Uncommon
755 emm Types in Thunder Bay, Ontario, Canada. *J Clin Microbiol* **54:**83-92.
756 27. **Flores AR, Luna RA, Runge JK, Shelburne SA, 3rd, Baker CJ.** 2017. Cluster of
757 Fatal Group A streptococcal *emm*87 infections in a single family: molecular basis for
758 invasion and transmission. *J Infect Dis* **215:**1648-1652.
759 28. **Alam FM, Turner CE, Smith K, Wiles S, Sriskandan S.** 2013. Inactivation of the
760 CovR/S virulence regulator impairs infection in an improved murine model of
761 *Streptococcus pyogenes* naso-pharyngeal infection. *PLoS One* **8:**e61655.
762 29. **Osowicki J, Azzopardi KI, McIntyre L, Rivera-Hernandez T, Ong CY, Baker C,**
763 **Gillen CM, Walker MJ, Smeesters PR, Davies MR, Steer AC.** 2019. A controlled
764 human infection model of group A *Streptococcus* pharyngitis: Which Strain and Why?
765 *mSphere* **4**.
766 30. **Rochefort A, Boukthir S, Moullec S, Meygret A, Adnani Y, Lavenier D, Faili A,**
767 **Kayal S.** 2017. Full sequencing and genomic analysis of three *emm*75 group A
768 *Streptococcus* strains recovered in the course of an epidemiological shift in French
769 Brittany. *Genome Announc* **5**.
770 31. **Sierig G, Cywes C, Wessels MR, Ashbaugh CD.** 2003. Cytotoxic effects of
771 streptolysin O and streptolysin S enhance the virulence of poorly encapsulated group A
772 streptococci. *Infect Immun* **71:**446-455.
773 32. **Lynskey NN, Goulding D, Gierula M, Turner CE, Dougan G, Edwards RJ,**
774 **Sriskandan S.** 2013. RocA truncation underpins hyper-encapsulation, carriage
775 longevity and transmissibility of serotype M18 group A streptococci. *PLoS Pathog*
776 **9:**e1003842.

33. **Moses AE, Wessels MR, Zalcman K, Alberti S, Natanson-Yaron S, Menes T, Hanski E.** 1997. Relative contributions of hyaluronic acid capsule and M protein to virulence in a mucoid strain of the group A *Streptococcus*. *Infect Immun* **65:**64-71.

34. **Flores AR, Jewell BE, Olsen RJ, Shelburne SA, 3rd, Fittipaldi N, Beres SB, Musser JM.** 2014. Asymptomatic carriage of group A *Streptococcus* is associated with elimination of capsule production. *Infect Immun* **82:**3958-3967.

35. **Flores AR, Chase McNeil J, Shah B, Van Beneden C, Shelburne SA, 3rd.** 2018. Capsule-negative *emm* types are an increasing cause of pediatric group A streptococcal infections at a large pediatric hospital in Texas. *J Pediatric Infect Dis Soc* doi:10.1093/jpids/piy053.

36. **Marks LR, Mashburn-Warren L, Federle MJ, Hakansson AP.** 2014. *Streptococcus pyogenes* biofilm growth in vitro and in vivo and its role in colonization, virulence, and genetic exchange. *J Infect Dis* **210:**25-34.

37. **Rendueles O, de Sousa JAM, Bernheim A, Touchon M, Rocha EPC.** 2018. Genetic exchanges are more frequent in bacteria encoding capsules. *PLoS Genet* **14:**e1007862.

38. **Ashbaugh CD, Alberti S, Wessels MR.** 1998. Molecular analysis of the capsule gene region of group A *Streptococcus*: the *hasAB* genes are sufficient for capsule expression. *J Bacteriol* **180:**4955-4959.

39. **Cole JN, Aziz RK, Kuipers K, Timmer AM, Nizet V, van Sorge NM.** 2012. A conserved UDP-glucose dehydrogenase encoded outside the *hasABC* operon contributes to capsule biogenesis in group A *Streptococcus*. *J Bacteriol* **194:**6154-6161.

40. **Tagini F, Aubert B, Troillet N, Pillonel T, Praz G, Crisinel PA, Prod'hom G, Asner S, Greub G.** 2017. Importance of whole genome sequencing for the assessment of outbreaks in diagnostic laboratories: analysis of a case series of invasive *Streptococcus pyogenes* infections. *Eur J Clin Microbiol Infect Dis* **36:**1173-1180.

41. **Lynskey NN, Turner CE, Heng LS, Sriskandan S.** 2015. A truncation in the regulator RocA underlies heightened capsule expression in serotype M3 group A streptococci. *Infect Immun* 83; 1732-33.

42. **Steer AC, Carapetis JR, Dale JB, Fraser JD, Good MF, Guilherme L, Moreland NJ, Mulholland EK, Schodel F, Smeesters PR.** 2016. Status of research and development of vaccines for *Streptococcus pyogenes*. *Vaccine* **34:**2953-2958.

43. **McShan WM, Nguyen SV.** (2016) The Bacteriophages of Streptococcus pyogenes. In: Ferretti JJ, Stevens DL, Fischetti VA, editors. *Streptococcus pyogenes : Basic Biology to Clinical Manifestations* [Internet]. Oklahoma City (OK): University of Oklahoma Health Sciences Center; 2016-. Available from: https://www.ncbi.nlm.nih.gov/books/NBK333409/

44. **Johnson DR, Kurlan R, Leckman J, Kaplan EL.** 2010. The human immune response to streptococcal extracellular antigens: clinical, diagnostic, and potential pathogenetic implications. *Clin Infect Dis* **50:**481-490.

45. **Reynolds R, Hope R, Williams L, Surveillance BWPoR.** 2008. Survey, laboratory and statistical methods for the BSAC Resistance Surveillance Programmes. *J Antimicrob Chemother* **62 Suppl 2:**ii15-28.

46. **Pospiech A, Neumann B.** 1995. A versatile quick-prep of genomic DNA from gram-positive bacteria. *Trends Genet* **11:**217-218.

47. **Page AJ, De Silva N, Hunt M, Quail MA, Parkhill J, Harris SR, Otto TD, Keane JA.** 2016. Robust high-throughput prokaryote de novo assembly and improvement pipeline for Illumina data. *Microb Genom* **2:**e000083.

48. **Stamatakis A.** 2014. RAxML version 8: a tool for phylogenetic analysis and post-analysis of large phylogenies. *Bioinformatics* **30:**1312-1313.

49. **Croucher NJ, Page AJ, Connor TR, Delaney AJ, Keane JA, Bentley SD, Parkhill J, Harris SR.** 2015. Rapid phylogenetic analysis of large samples of recombinant bacterial whole genome sequences using Gubbins. *Nucleic Acids Res* **43:**e15.

50. **Letunic I & Bork P. 2019.** Interactive Tree Of Life (iTOL) v4: recent updates and new developments. *Nucleic Acids Research.* **47:**W256–W259

51. **Bolger AM, Lohse M, Usadel B.** 2014. Trimmomatic: a flexible trimmer for Illumina sequence data. *Bioinformatics* **30:**2114-2120.

52. **Arndt D, Grant J, Marcu A, Sajed T, Pon A, Liang Y, Wishart DS** (2016) PHASTER: a better, faster version of the PHAST phage search tool. *Nucleic Acids Research*. **44:**W16-21

53. **Inouye M, Dashnow H, Raven LA, Schultz MB, Pope BJ, Tomita T, Zobel J, Holt KE.** 2014. SRST2: Rapid genomic surveillance for public health and hospital microbiology labs. *Genome Med* **6:**90.

54. **Gupta SK, Padmanabhan BR, Diene SM, Lopez-Rojas R, Kempf M, Landraud L, Rolain JM.** 2014. ARG-ANNOT, a new bioinformatic tool to discover antibiotic resistance genes in bacterial genomes. *Antimicrob Agents Chemother* **58:**212-220.

55. **Remmington A, Turner CE.** 2018. The DNases of pathogenic Lancefield streptococci. *Microbiology*. **164:**242-250.

Tables

Table 1. Three key residue variants within the *nga-ifs-slo* promoter

Promoter variant	Type	Genotype (% of isolates)
$A_{-27}T_{-22}C_{-18}$	1.1	**4 (1)***, 8 (100), **9 (92)**, 11 (100), **22 (3)**, **25 (33)**, **28 (87.7)**, 33 (100), 41 (100), 43 (100), **44 (9)**, 49 (100), 53 (100), **58 (15)**, 60 (100), 63 (100), **75 (9)**, **76 (41)**, **77 (29)**, **81 (23)**, **82 (1)**, **88 (33)**, **89 (1)**, **90 (4)**, 92 (100), **94 (6)**, 101 (100), **102 (50)**, **103 (17)**, 106 (100), **108 (89)**, 110 (100), 113 (100), 151 (100), 168 (100), 232 (100)
	1.2	9(8)
	1.3	88(67)
$G_{-27}T_{-22}T_{-18}$	2.1	5 (100), 6 (100), 18 (100), **25 (67)**, **44 (28)**, 68 (100), **75 (1)**, **76 (5), 77 (1), 82 (1), 87 (2), 89 (6), 90 (96),** 91 (100)**, 102 (50), 103 (83),** 104 (100),
	2.2	118 (100) 2 (100), 27 (100), **44 (62)**, **58 (85)**, 59 (100), 73 (100), **76 (11)**, **77 (36)**, **82 (89)**, 83 (100)
	2.3	32 (100)
$A_{-27}G_{-22}T_{-18}$	3.1	1(100), 3 (100), 12 (100), **22 (97)**, **75 (90)**, **76 (43)**, **81 (77)**, **82 (9)**, **89 (93)**, **94 (94)**, **108 (11)**
	3.2	**4 (99), 28 (0.3), 77 (34)**, **87 (98)**
$A_{-27}T_{-22}T_{-18}$	4	**28 (12)**, 78 (100)

* genotypes in bold have more than one variant within the population

Figure Legends

Figure 1. Low diversity within *emm* genotypes. (**A**) A maximum likelihood phylogenetic tree constructed from 113,805 core SNPs extracted after mapping all 344 BSAC isolates to the complete *emm*89 reference strain H293 (indicated by a star), identified that the majority of isolates cluster by *emm* genotype. Exceptions were *emm*44, *emm*90 and *emm*101 (highlighted with black dots), each of which were present as two separate lineages. Branches are coloured based on bootstrap support (scale bar in figure). Boxes at branch tips are coloured by *emm*-type and the *emm*-type numbers are provided around the outside of the tree. (**B**) As reflected by the phylogenetic tree, the number of SNPs separating isolates was high (>5000) when the genomes of isolates of different *emm*-types were compared (black bars). This was much lower when comparisons were made between the genomes of isolates of the same *emm*-type (red bars).

Figure 2. Comparison of the variation within the P-*nga*-*ifs*-*slo* region and core chromosome. A maximum likelihood phylogenetic tree was constructed from 205 SNPs extracted from an alignment of the *nga*-*ifs*-*slo* locus and associated upstream region to include the promoter (P-*nga*-*ifs*-*slo*) extracted from *de novo* assemblies of BSAC *S. pyogenes* collection (Left tree). This was compared to the phylogenetic tree constructed using 75,851 SNPs across the entire core genome after mapping to the H293 reference genome (Right tree). Only 20 of the most common *emm* genotypes were included; *emm*1, 3, 4, 5, 6, 12, 18, 22, 28, 43, 44, 75, 76, 77, 78, 81, 83, 87, 89, 101 (n=303 isolate genomes). Numbers and coloured blocks on the right tree represent *emm*-type. Variants of the P-*nga*-*ifs*-*slo* are of the same colour to *emm*-type if unique to that *emm*-type. The P-*nga*-*ifs*-*slo* variant found in *emm*1 (red) was common to other genotypes *emm*12, *emm*22 and some *emm*89. The genotypes *emm*76, *emm*87 and *emm*89 were linked to more than one variant of P-*nga*-*ifs*-*slo*. Grey shading indicates high expressing promoter variants; $A_{-27}T_{-22}T_{-18}$ (top) or $A_{-27}G_{-22}T_{-18}$

(bottom). Other non-shaded are low expressing promoter variants $A_{-27}T_{-22}C_{-18}$ or $G_{-27}T_{-22}T_{-18}$. Scale bar represents substitution per site. Bootstrap support values are provided on branches.

Figure 3. Variants of the *nga-ifs-slo* promoter. (A) The three key residues predicted to influence promoter activity are highlighted blue with those associated with high activity in red. We identified four combinations of these residues (four promoter types) with subtype variants differing in residues other than -27, -22 and -18 (residue positions relative to the underlined -35 and -10 regions) in the predicted 67bp promoter region (9). The combination of $A_{-27}T_{-22}C_{-18}$ subtype 1.1 in historical *emm*1 and $G_{-27}T_{-22}T_{-18}$ subtype 2.1 in older *emm*89 have been shown to be associated with low level promoter activity. $A_{-27}G_{-22}T_{-18}$ subtype 3.1 promoter in modern *emm*1 and emergent variant *emm*89 has been shown to have high activity. $A_{-27}T_{-22}T_{-18}$ subtype 4 promoter has also been shown to have high activity in *emm*28 (11). Subtypes 1.2, 1.3 and 2.3 were restricted to *emm*9, *emm*88 and *emm*32 strains respectively. **(B)** Weblogo representation of the variability in the 67bp promoter region of *nga/ifs/slo* within the 54 different *emm*-types. Key residues -27, -22, -18 are highlighted (star) and their positions are relative to the -35 and -10 boxes. Figure generated using weblogo.berkeley.edu.

Figure 4. Non-functional mutations within the capsule locus genes. The *hasABC* genes were extracted from the assembled genomes of BSAC, CUH, PHE-2015/15, and ABCs-2015 isolate collections, and polymorphisms or indels leading to nonsense mutations and premature stop codons were identified, as well as gene absence. The percentage of isolates with full length (grey), truncated (red) or absent (black) HasA, HasB or HasC is depicted for each of the 54 *emm*-types. *emm*-types with fewer than 3 isolates were excluded. N = 5271 isolates genomes shown. Mutations in HasA were detected in more than 50% of isolates belonging to genotypes *emm*8 (n=3/4), *emm*11 (n=63/108), *emm*25 (n=2/3), *emm*27 (n=3/3), *emm*28 (n=358/363), *emm*58 (n=21/33), *emm*68 (n=12/14), *emm*73 (n=25/27), *emm*77

(n=72/80), *emm*78 (n=8/8), *emm*87 (n=119/121) and *emm*102 (n=6/6). Mutations in HasB were detected in 100% of *emm*94 isolates (n=54/54) and 60-77% of *emm*63 (n=3/5), *emm*81 (n=50/65) and *emm*90 (n=16/26) isolates.

Figure 5. Regions of recombination spanning the P-*nga*-*ifs*-*slo* locus. Recombination across the *nga*, *ifs* and *slo* genes (blue arrows) was identified in eight genotypes in addition to the previously described *emm*1 and *emm*89. Length of recombination, predicted by SNP cluster analysis, ranged from ~6kb to 36kb. With the exception of *emm*75, all regions also encompassed the promoter of *nga*-*ifs*-*slo*. All regions are shown relative to a ~40kb region within the reference genome H293 and genes within this region are depicted as arrows. Recombination in *emm*1 extended beyond that depicted here and is shown as a broken line.

Figure 6. Recombination within the *emm*28 and *emm*87 populations. **(A)** Maximum likelihood phylogeny constructed with 33,537 core SNPs following mapping of all available *emm*28 genome data to the *emm*28 MGAS6180 reference genome (white square) (18). Modern UK isolates (red circles); BSAC (n=15), CUH (n=13 (12)) and PHE-2014/15 (n=240 (13, 14)), one historical English isolate from 1938 (brown square). North American isolates (blue circles); ABCs-2015 (n=95 (15)), Canada (2011-2013, n=4 (20)), and completed genome strain HarveyGAS (USA, 2017 (21)). Other isolates; Lebanon (n=1, orange circle (22)), Australia (n=5, green circles (23)), France (STAB10015 (24), M28PF1 (25), turquoise circles). Total number of isolate genomes was 379. Two lineages of *emm*28 were identified, one clustering with MGAS6180 (white square) and the other (shaded grey) clustering with MEW123 (2012 USA (19), white circle). (**B)** Regions of recombination were then identified within the *emm*28 genome alignment and removed before reconstructing a phylogenetic tree using 17,885 variable sites (**C**) Maximum likelihood phylogeny constructed with 6,292 core SNPs following mapping of all available *emm*87 genome sequence data to the reference *emm*87 strain NGAS743 (Canada, white circle (26)). UK isolates (red circles); BSAC (2001-

926 2011, n=22), CUH (2008, n=1 (12)), PHE-2014/15 (n=72, (13, 14)). North American isolates
927 (blue circles); ABCs-2015 (n=26, (15)), Canada (n=23, (20, 26)), Texas Children's Hospital
928 (2012-2016, n=27, (27)). NCTC12065 (Genbank accession number GCA_900460075.1)
929 isolate from ~1970-80s was also included (brown square). Total number of isolates was 173.
930 Three isolates (shaded grey) were distinct from the main population. The branch was
931 shortened for one isolate for presentation purposes. (**D**) Regions of recombination were
932 identified within the *emm*87 genome alignment and removed before reconstructing a
933 phylogenetic tree using 1,531 variable sites. Isolates indicated by * in both *emm*28 and
934 *emm*87 populations were predicted to have undergone recombination in regions surrounding
935 the *hasABC* locus. Scale bars represents single nucleotide polymorphisms. PHE-2014/15
936 *emm*28 isolates GASEMM1261, GASEMM2648, GASEMM1396 and GASEMM1353 were
937 removed for presentation purposes as they represented highly divergent lineages.

938 **Figure 7. Two lineages within *emm*75. (A)** Maximum likelihood phylogeny constructed
939 with 9,241 core SNPs following mapping of all available *emm*75 genome sequence data to
940 the genome of French strain STAB090229 (white circle) (30). Modern UK collections (red
941 circles); BSAC (n=11), CUH (n=6 (12)), PHE-2014/15 (n = 141, (13, 14)) and two English
942 historical isolates (brown squares) from 1937/1938. North American isolates (blue circles);
943 ABCs-2015 (n=20, (15)), NGAS344 and NGAS604 from Canada 2011/2012 (26). French
944 strains (turquoise circles); STAB120304 (2012) and STAB14018 (2014) (30). Total number
945 of isolates was 185. Two lineages were identified, generally characterised by the MLST;
946 ST49 (shaded grey) or ST150 (with minor MSLT variants ST788, ST851, ST861 within these
947 lineages). (**B)** Gubbins analysis identified ten regions of predicted recombination (red lines)
948 in all modern ST49 compared to historical 1930s ST49 across the genome (indicated across
949 the top). One region included P-*nga*-*ifs*-*slo* (shaded grey). The phylogenetic tree was
950 constructed with 1,953 variable sites following removal of predicted regions of

recombination. Scale bars represent single nucleotide polymorphisms. One PHE-2014/15 isolates (GASEMM1722) was excluded for presentation purposes as it was highly divergent from the rest of the population.

Figure 8. Variants of P-*nga*-*ifs*-*slo* and capsule mutations associated with lineages of *emm*76, *emm*77 and *emm*81. Maximum likelihood phylogeny identified multiple sequence type (ST) lineages within the populations of (**A**) *emm*76, (**B**) *emm*77 and (**C**) *emm*81. Collection indicates either BSAC or CUH (dark red), PHE-2014/15 isolates (red), ABCs-2015 (blue) or English historical (brown). Dates for BSAC, CUH or historical are shown; other isolates were from 2014/2015. STs are indicated on the right and major lineages shaded grey. **(A)** Genome data for *emm*76 was mapped to the *de novo* assembled sequence of BSAC_bs448 from 2002, selected as the oldest isolate representing the genotype. Genome data from a total of 38 isolates was used; BSAC (n=2), PHE-2014/15 (n=18, (13, 14)), ABCs-2015 (n=18 (15)). Predicted prophage regions were removed and a maximum likelihood phylogenetic tree constructed from 30,264 core SNPs. Five STs were identified (indicated on right of tree) but the main lineage was ST50. (**B**) All *emm*77 genome data was mapped to the *de novo* assembled sequence of BSAC_bs150 from 2001. Genome data from a total of 80 isolates were used; BSAC (n=5), PHE-2014/15 (n=21 (13, 14)), ABCs-2015 (n=54 (15)). Four STs were identified but the main lineage was ST63, with one isolate in this lineage being single locus variant ST1125. Predicted prophage regions were removed and a maximum likelihood phylogenetic tree constructed from 34,760 core SNPs. (**C**) All *emm*81 genome data was mapped to the *de novo* assembled seqeunce of BSAC_bs229 from 2001. Genome data from a total of 68 isolates were used; *emm*81; BSAC (n=9), CUH (n=1, (12)), PHE-2014/15 (n=29 (13, 14)), ABCs-2015 (n=26 (15)), English historical 1930s (n=3). Predicted prophage regions were removed and a maximum likelihood phylogenetic tree constructed from 42,258 core SNPs. Nine STs were identified but the main lineage was

976 ST624 with and minor (single base change in *recP*) ST variant ST837. We identified variants
977 of P-*nga*-*ifs*-*slo* (P) associated with one of three combinations of key promoter residues
978 including the high activity associated $A_{-27}G_{-22}T_{-18}$ (P; black). For (**A**) *emm*76 and (**B**) *emm*77,
979 mutations were detected in *hasA* predicted to truncate HasA (H; black). All (**C**) *emm*81
980 isolates were predicted to express full length HasA but the ST624/ST837 lineage carry a
981 mutation within *hasB* leading to a truncated HasB (H; grey). Branches are coloured based on
982 bootstrap support (scale bar provided). Scale bars represent substitutions per site. Isolates
983 used as references for mapping indicated with black circles. Branches for lineages outside
984 main lineages were shortened for presentation purposes (indicated by line breaks). C;
985 collection, P; promoter key residue combination, H; Full length or truncated HasA or HasB.
986

Supplementary Material

Table S1. Reference genomes used for mapping to in this study and excluded prophage regions

Dataset S1. Details of BSAC isolates and antimicrobial sensitivity testing

Dataset S2. Details of all isolates with assembly statistics, capsule gene mutations and *nga/ifs/slo* promoter variants.

Dataset S3. Details of *emm*28, *emm*75, *emm*76, *emm*77, *emm*81, *emm*87, *emm*94 and *emm*108 isolates used in this study.

Figure S1. Number of isolates per *emm*-type in the BSAC collection. Forty-four different genotypes were identified within the collection but 16 were represented by single isolates (grey bars). Total number of isolates was 344.

Figure S2. NADase activity of different promoter subtypes. The activity of NADase was measured in culture supernatant of BSAC isolates representing different promoter subtypes with predicted low (black) or high (red) activity. $A_{-27}T_{-22}C_{-18}$ subtype 1.1 promoter had low activity in *emm*81 isolates, consistent with previous findings of this promoter in historical *emm*1. $G_{-27}T_{-22}T_{-18}$ subtype 2.1 had low activity in older *emm*89, also consistent with previous findings, and subtype 2.2 in *emm*58 and *emm*77 also had low activity, as predicted despite the additional base change at -40bp. Compared to $G_{-27}T_{-22}T_{-18}$ subtype 2.1 (older *emm*89), significantly higher activity was detected in *emm*1, with $A_{-27}G_{-22}T_{-18}$ subtype 3.1, and in *emm*4 and *emm*87 with subtype 3.2, also supporting a null effect of the base change at -40bp. $A_{-27}T_{-22}T_{-18}$ subtype 4 promoter in *emm*78 also had significantly higher activity. Isolates with mutations in regulators *covR*/S or *rocA* were excluded as they influence the expression of *nga*. Data represent mean +SD of e*mm*1; n=10, *emm*89; n=11, *emm*58; n=3, *emm*77; n=3, *emm*4; n=7, *emm*87; n=17, *emm*78; n=5, *emm*81; n=5. Statistical comparisons were made to

*emm*89 subtype 2.1, for which we had the highest number of representative isolates and was previously confirmed to have low activity, using Kruskal-Wallis non-parametric multiple comparison test; * $p<0.05$, ** $p<0.01$, *** $p<0.001$, non-significant (n.s).

Figure S3. Recombination within ST50 *emm*76. All sequence data for *emm*76 (n=38) was mapped the *de novo* assembled sequence of BSAC_bs448 (bold). The majority of isolates were ST50 (ST; white) and within this ST were two sub-lineages; the lower sub-lineage was associated the high activity promoter $A_{-27}G_{-22}T_{-18}$ (P; black) and truncated HasA (HasA/B; black). Gubbins analysis (boxed region on right) of ST50 isolates identified 19 regions of recombination across the genome in all isolates (red vertical lines) belonging to the lower sub-lineage compared to the top sub-lineage. One of these regions (highlighted grey) surrounded the P-*nfa-ifs-slo* locus conferring the high activity associated promoter (P; black) with residues $A_{-27}G_{-22}T_{-18}$ to the lower sub-lineage compared to low activity $A_{-27}T_{-22}C_{-18}$ (P; grey) in the top sub-lineage. The presence (black) or absence (white) of mobile prophage-associated superantigens (*speA, C, H, I, K, L, M, ssa*) and DNAses (*sda, sdn, spd1, spd3, spd3v6, spd4*) as well as antimicrobial resistance genes and mutant variants of regulators CovR, CovS and RocA was also determined for each isolate. All isolates within the lower ST50 sub-lineage carried a variant of the prophage-associated DNAse *spd3* (*spd3v6*) (54) that is more divergent than other *spd3* variants, including the *spd3* variant carried by isolates belonging to the top ST50 sub-lineage. All lower sub-lineage isolates also carried the resistance gene *ermB* which was absent in other lineages, but they did not carry other antimicrobial elements found in the upper sub-lineage isolates. Sporadic truncated mutant variants of regulators CovR, CovS and RocA (black) were also detected across the tree but were not associated with any specific lineages. Scale bar represents substitutions per site. Scale on boxed region represents position across the assembled BSAC_bs448 genome. Bootstrap values provided on major branches.

Figure S4. Recombination within ST63 *emm*77. All sequence data for *emm*77 (n=82) was mapped to the *de novo* assembled sequence of BSAC_bs150 (bold). The majority of isolates were ST63 (ST; white), or one single locus variant ST1125, and within this ST were two sub-lineages; the upper lineage associated with the high activity promoter $A_{-27}G_{-22}T_{-18}$ (P; black) and truncated HasA (H; black). Gubbins analysis (boxed region) of ST63 isolates identified two regions of recombination across the genome of all isolates (red vertical lines) belonging to the upper sub-lineage compared to the lower sub-lineage. One of these regions (highlighted grey) surrounded the P-*nfa*-*ifs*-*slo* locus conferring the high activity associated promoter with residues $A_{-27}G_{-22}T_{-18}$ (P; black) to the upper sub-lineage compared to low activity $G_{-27}T_{-22}T_{-18}$ (P; white) in the lower sub-lineage. The presence (black) or absence (white) of mobile prophage-associated superantigens (*speA, C, H, I, K, L, M, ssa*) and DNAses (*sda, sdn, spd1, spd3, spd3v6, spd4*) as well as antimicrobial resistance genes and truncated mutant variants of regulators CovR, CovS and RocA was also determined for each isolate. The prophage associated DNase *spd*3 was common to all upper sub-lineage ST63 and all except one of this sub-lineage carried the antimicrobial resistance gene *ermTR*. Sporadic truncated mutant variants of CovR, CovS and RocA (black) were detected across the tree but were not associated with any specific lineages. Scale bar represents substitutions per site. Scale on boxed region represents position in the BSAC_bs150 assembly. Bootstrap values provided on main branches.

Figure S5. Recombination within *emm*81. All sequence data for *emm*81 (n=68) was mapped to the *de novo* assembled sequence of BSAC_bs229 (bold). The majority of isolates were ST624, with high activity promoter $A_{-27}G_{-22}T_{-18}$ (P; black) and truncated HasB (HasB; black). Gubbins analysis (boxed region) of ST624 isolates and closely related ST1059, ST117, ST909 and ST837, compared to BSAC_bs229, identified patterns of recombination across the genome in all isolates (red vertical lines, or blue vertical lines if unique to a single

isolate). One of these regions (highlighted grey) surrounded the P-*nfa-ifs-slo* locus conferring the high activity associated promoter with residues $A_{-27}G_{-22}T_{-18}$ to the ST624/ST837 population compared to low activity $G_{-27}T_{-22}T_{-18}$ in all other isolates. The presence (black) or absence (white) of mobile prophage-associated superantigens (*speA, C, H, I, K, L, M, ssa*) and DNAses (*sda, sdn, spd1, spd3, spd3v6, spd4*) as well as antimicrobial resistance genes and truncated mutant variants of regulators CovR, CovS and RocA was also determined for each isolate. The majority of all isolates carried the prophage-associated *speH*. Antimicrobial resistance genes were rarely detected in any ST. Scale bar represents substitutions per site. Scale on boxed region represents position in the BSAC_bs229 assembly. Bootstrap values provided on main branches.

Figure S6. Recombination in *emm*94 and *emm*108. (A) In the PHE-2014/2015 (red) *emm*94 population, the majority (n=51) form a lineage separate from two PHE-2014/2015 isolates and the single ABCs-2015 (blue) isolate. Gubbins analysis predicted 11 regions of recombination (red lines) in all the lineage associated isolates compared to the three other isolates. One of these regions (highlighted in grey) encompassed the P-*nga-ifs-slo* region. (**B**) Isolates of *emm*108 from the ABCs-2015 (blue) collection were of a different MLST (ST14) compared to PHE-2014/15 (red) (ST1088). The *hasB* gene was absent in the genomes of both ABCs-2015 isolates and one had undergone recombination surrounding the P-*nga-ifs-slo* locus (shaded grey), as predicted by Gubbins analysis (shown on the right). Blue lines; predicted recombination unique to a single genome. Sequence data were mapped to the reference strain H293, also used as an outgroup for SNP cluster analysis. Scale bar represents SNPs.

Figure 1

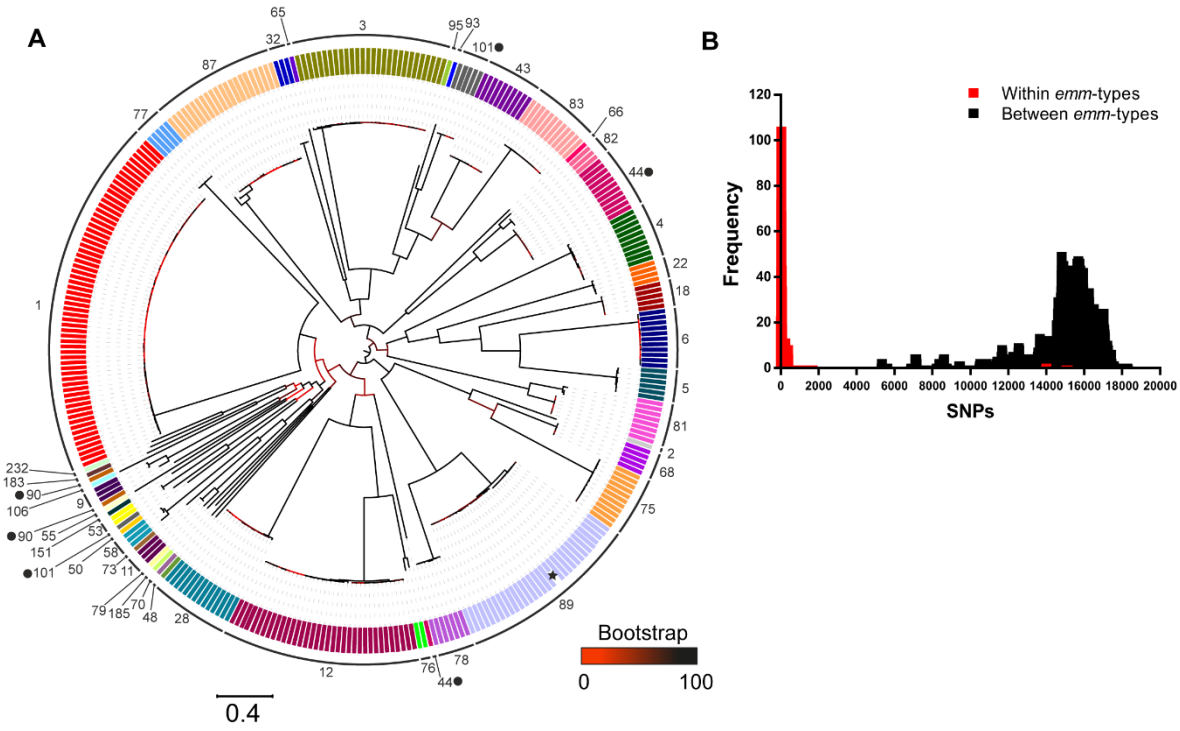
A
B
Bootstrap
0
100
0.4
Within emm-types
Between emm-types
Frequency
SNPs
0
20
40
60
80
100
120
0
2000
4000
6000
8000
10000
12000
14000
16000
18000
20000

Figure 2

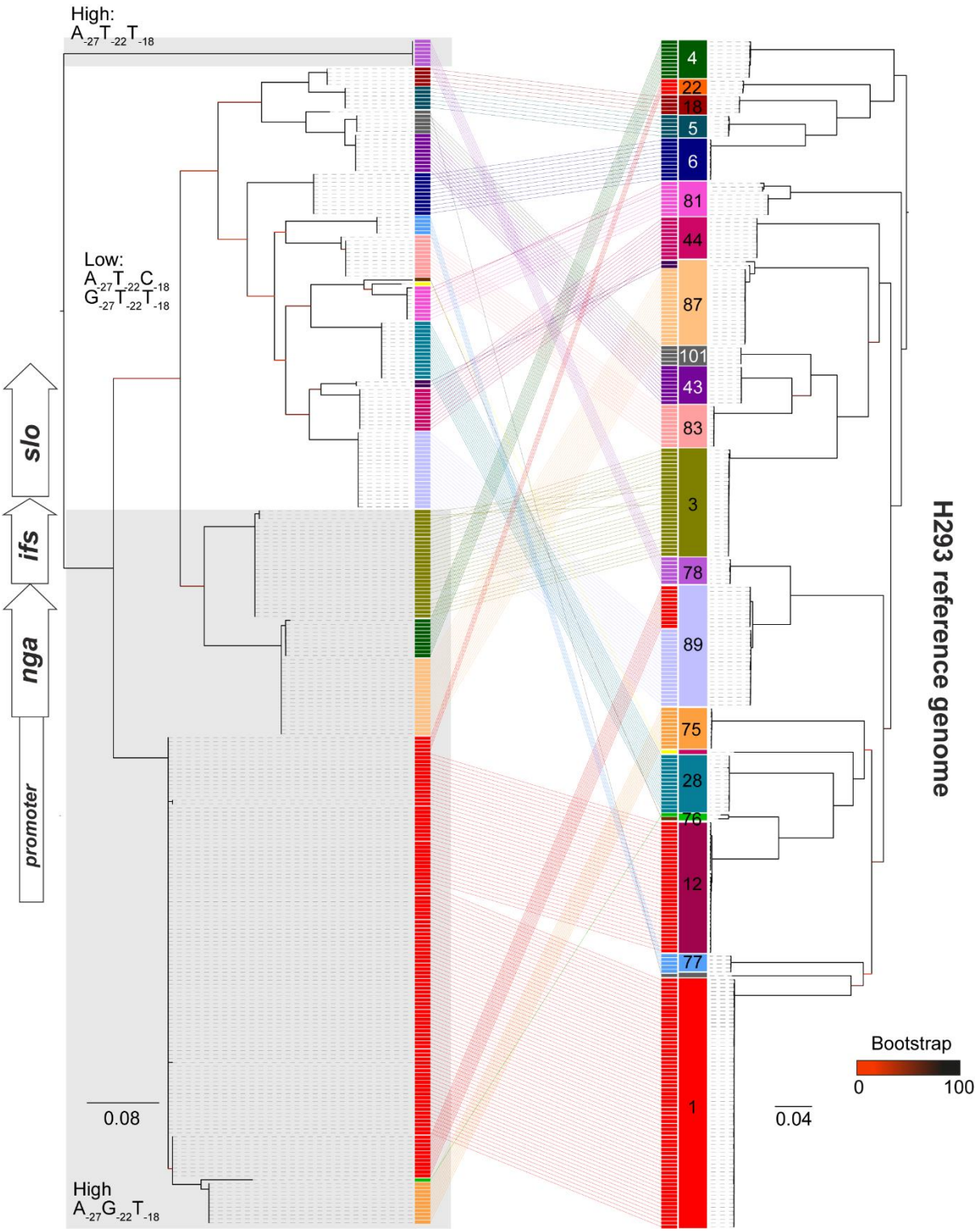
High:
A-27T-22T-18
Low:
A-27T-22C-18
G-27T-22T-18
High
A-27G-22T-18
slo
ifs
nga
promoter
0.08
0.04
4
22
18
5
6
81
44
87
101
43
83
3
78
89
75
28
76
12
77
1
H293 reference genome
Bootstrap
0
100

Figure 3

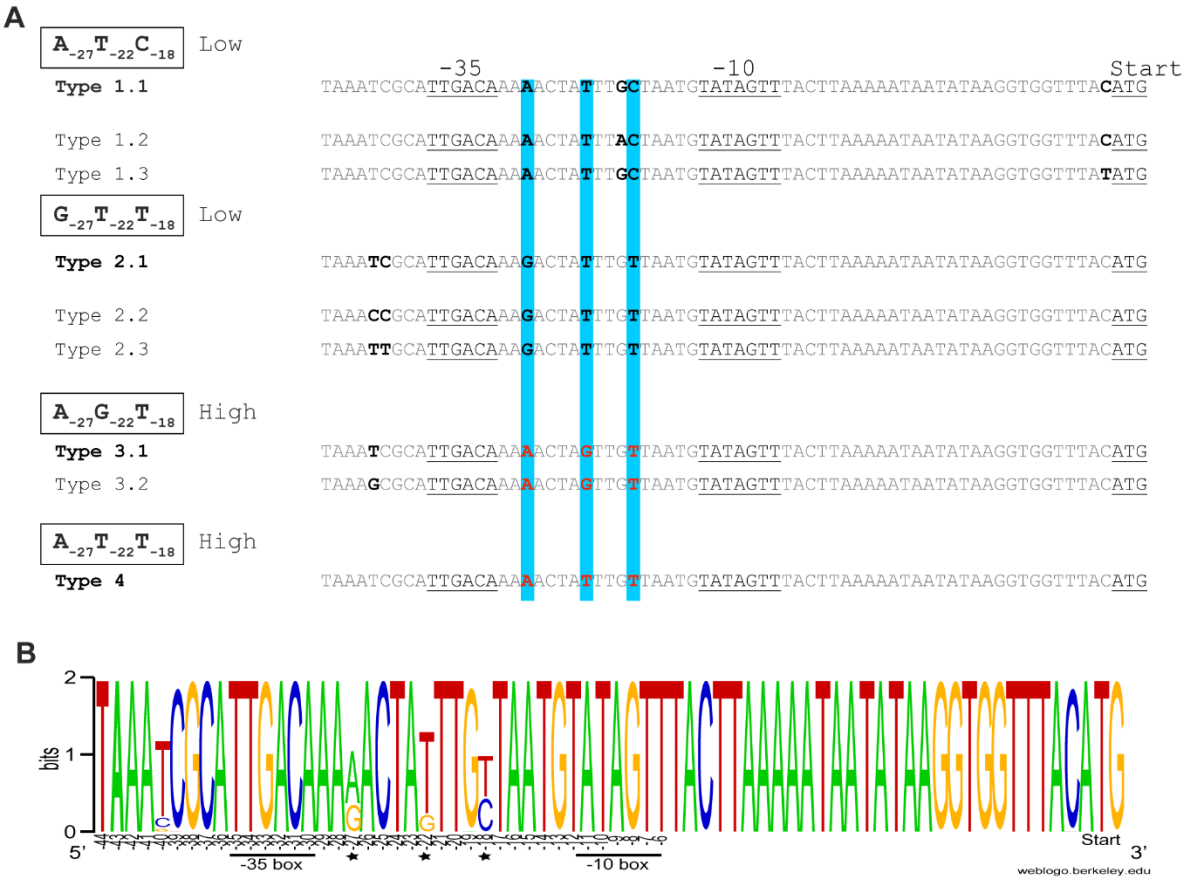
A
A-27T-22C-18
Low
-35
-10
Start
Type 1.1
TAAATCGCATTGACAAAAACTATTTGCTAATGTATAGTTTACTTAAAAATAATATAAGGTGGTTTACATG
Type 1.2
TAAATCGCATTGACAAAAACTATTTACTAATGTATAGTTTACTTAAAAATAATATAAGGTGGTTTACATG
Type 1.3
TAAATCGCATTGACAAAAACTATTTGCTAATGTATAGTTTACTTAAAAATAATATAAGGTGGTTTATATG
G-27T-22T-18
Low
Type 2.1
TAAATCGCATTGACAAAGACTATTTGTTAATGTATAGTTTACTTAAAAATAATATAAGGTGGTTTACATG
Type 2.2
TAAACCGCATTGACAAAGACTATTTGTTAATGTATAGTTTACTTAAAAATAATATAAGGTGGTTTACATG
Type 2.3
TAAATTGCATTGACAAAGACTATTTGTTAATGTATAGTTTACTTAAAAATAATATAAGGTGGTTTACATG
A-27G-22T-18
High
Type 3.1
TAAATCGCATTGACAAAAACTAGTTGTTAATGTATAGTTTACTTAAAAATAATATAAGGTGGTTTACATG
Type 3.2
TAAAGCGCATTGACAAAAACTAGTTGTTAATGTATAGTTTACTTAAAAATAATATAAGGTGGTTTACATG
A-27T-22T-18
High
Type 4
TAAATCGCATTGACAAAAACTATTTGTTAATGTATAGTTTACTTAAAAATAATATAAGGTGGTTTACATG
B
bits
2
1
0
5'
3'
Start
-35 box
-10 box
weblogo.berkeley.edu

1097 **Figure 4**

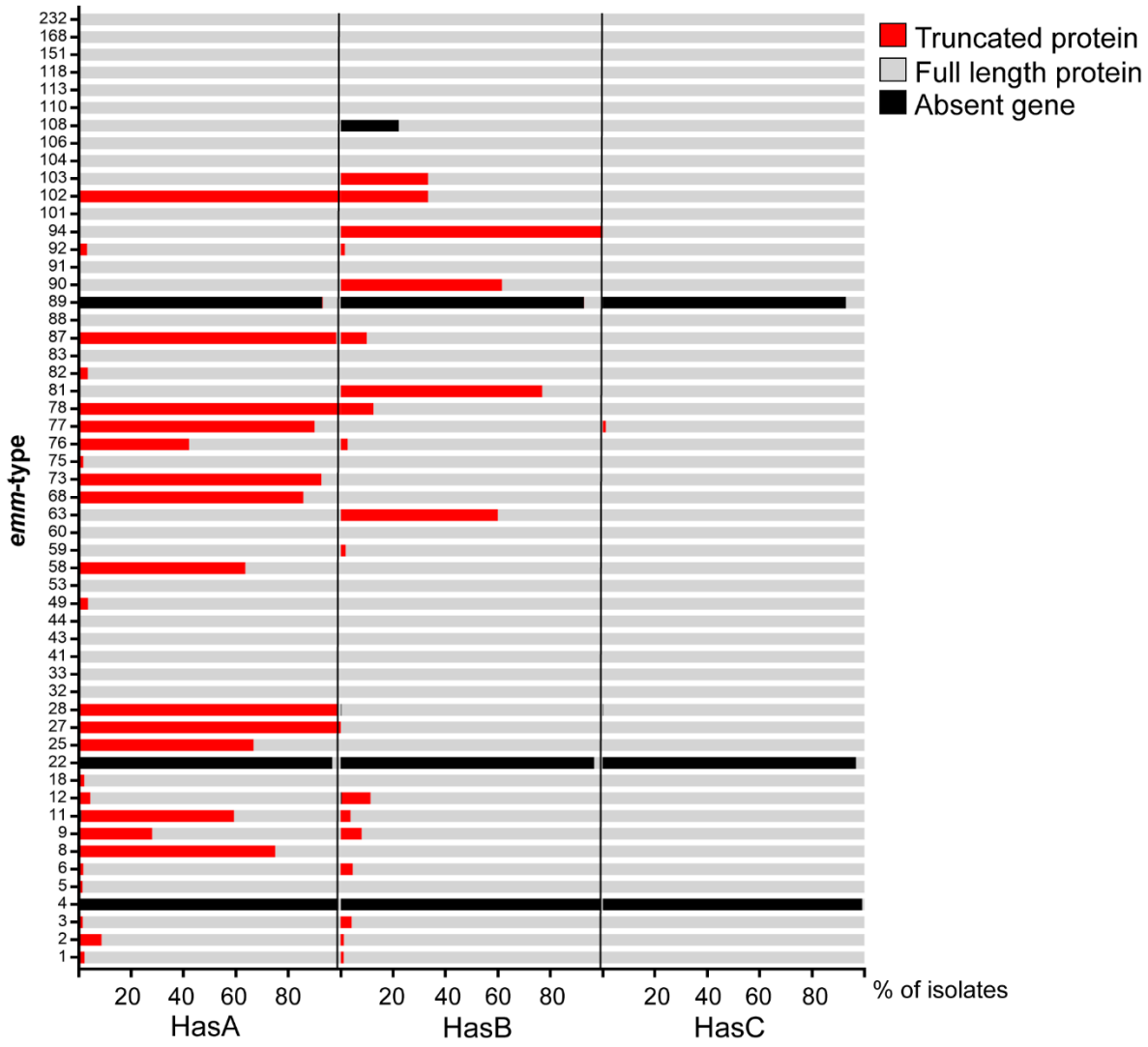

1098

1099

Figure 5

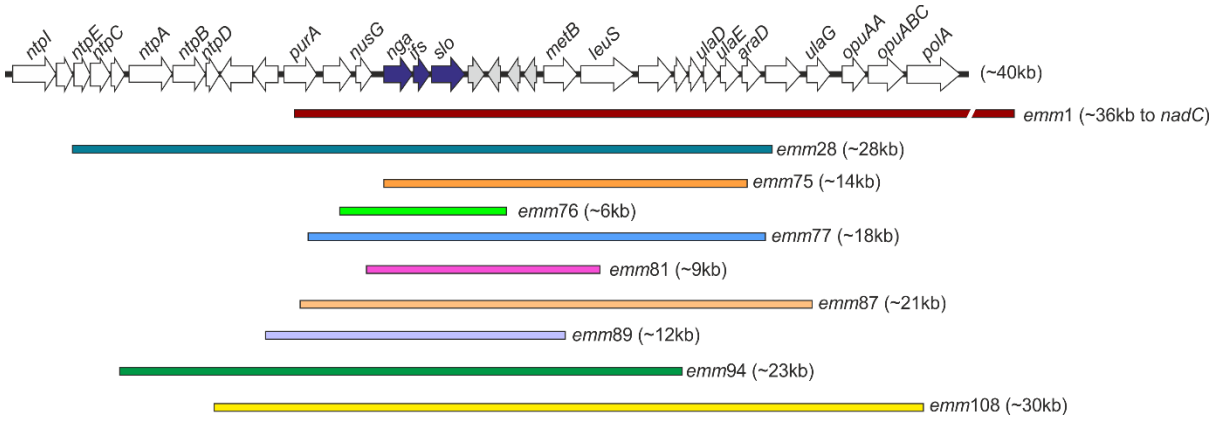
ntpI
ntpE
ntpC
ntpA
ntpB
ntpD
purA
nusG
nga
ifs
slo
metB
leuS
ulaD
ulaE
araD
ulaG
opuAA
opuABC
polA
(~40kb)
emm1 (~36kb to nadC)
emm28 (~28kb)
emm75 (~14kb)
emm76 (~6kb)
emm77 (~18kb)
emm81 (~9kb)
emm87 (~21kb)
emm89 (~12kb)
emm94 (~23kb)
emm108 (~30kb)

Figure 6

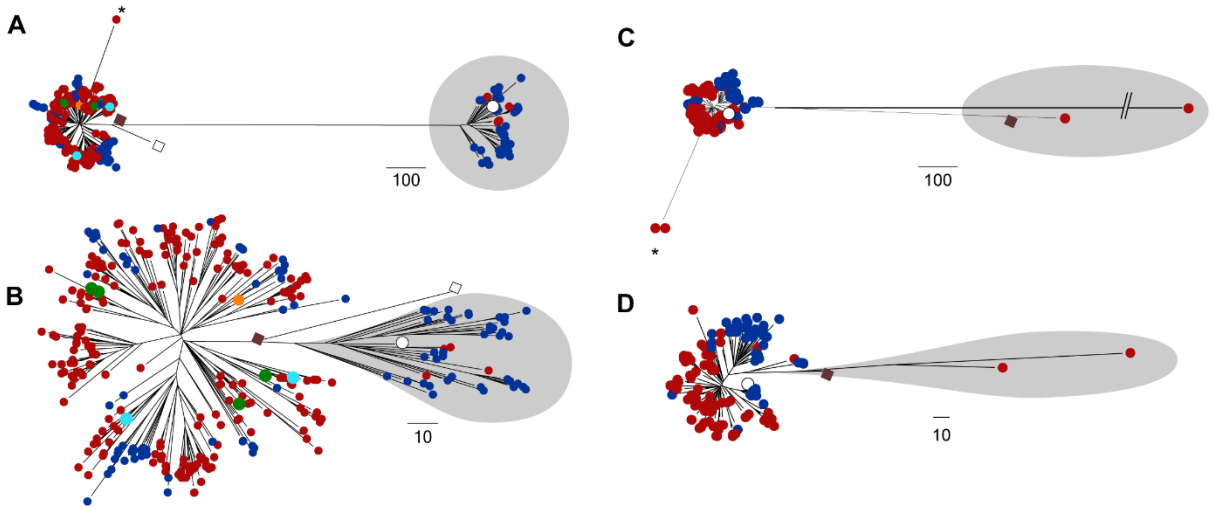

1107 **Figure 7**

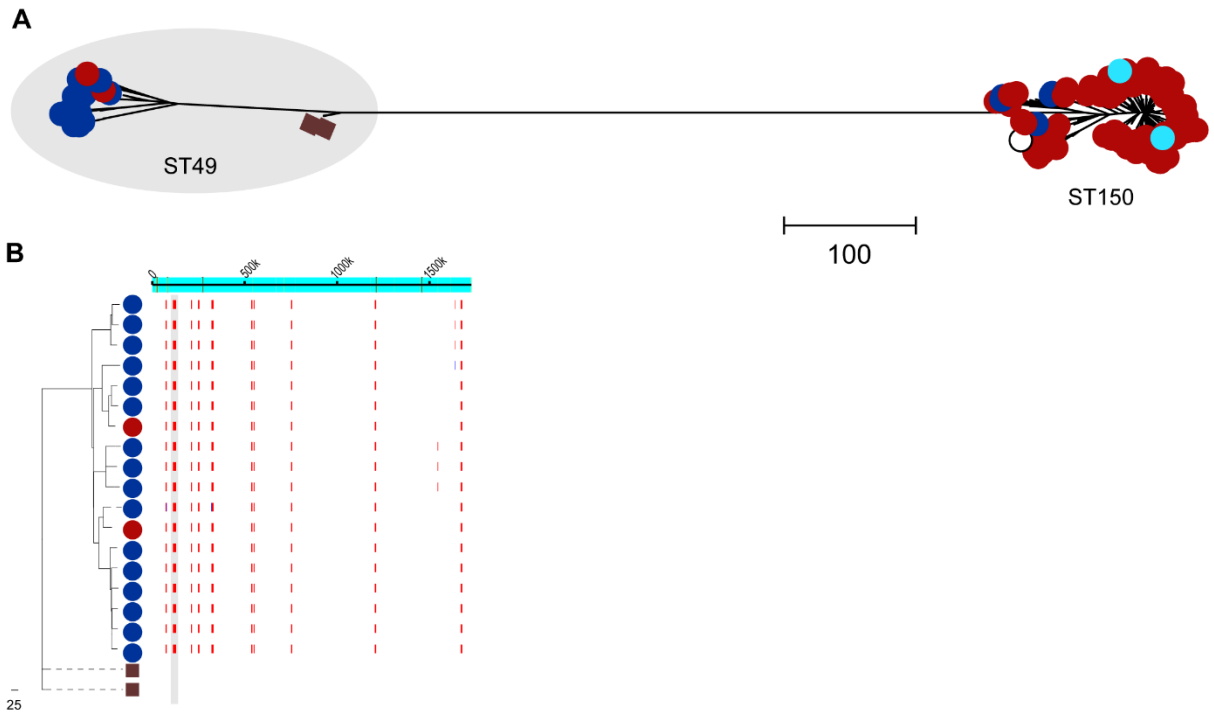

1108

1109

1110 **Figure 8**

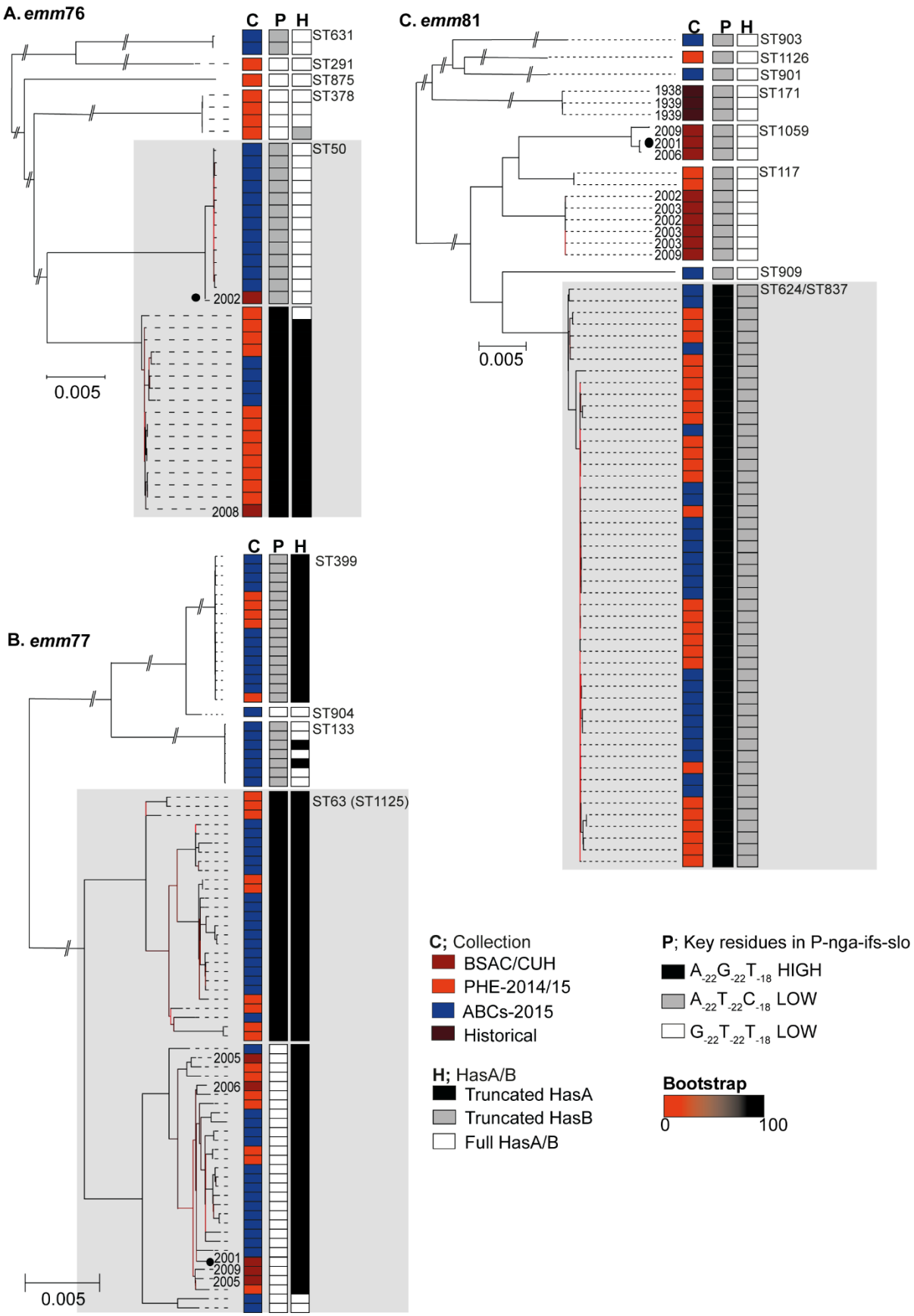

1111

Figure S1

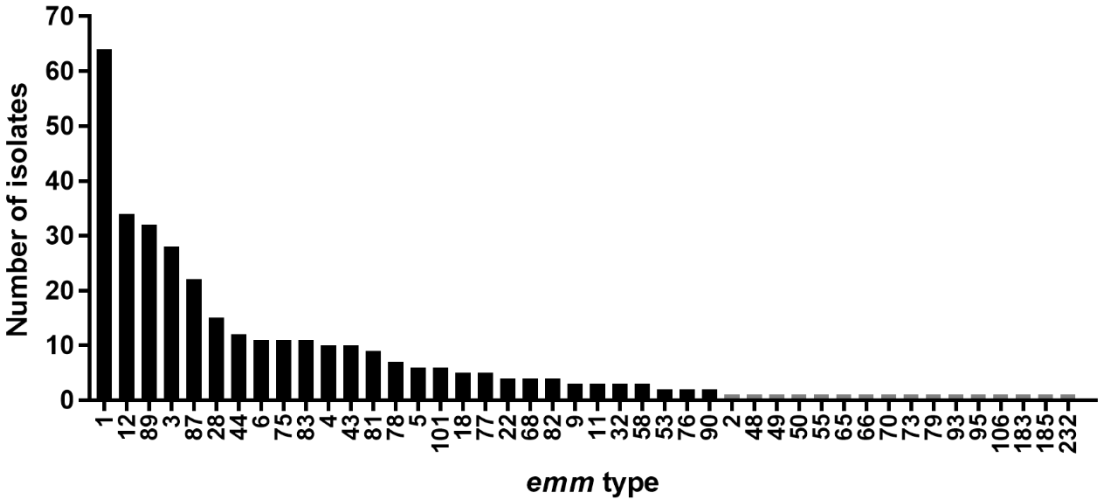
Number of isolates
70
60
50
40
30
20
10
0
1
12
89
3
87
28
44
6
75
83
4
43
81
78
5
101
18
77
22
68
82
9
11
32
58
53
76
90
2
48
49
50
55
65
66
70
73
79
93
95
106
183
185
232
emm type

Figure S2

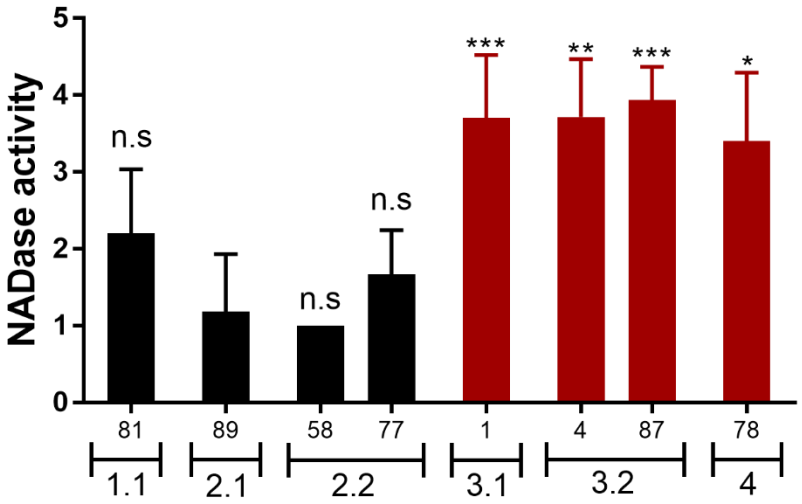
NADase activity
5
4
3
2
1
0
n.s
n.s
n.s
***
**
***
*
81
89
58
77
1
4
87
78
1.1
2.1
2.2
3.1
3.2
4

Figure S3

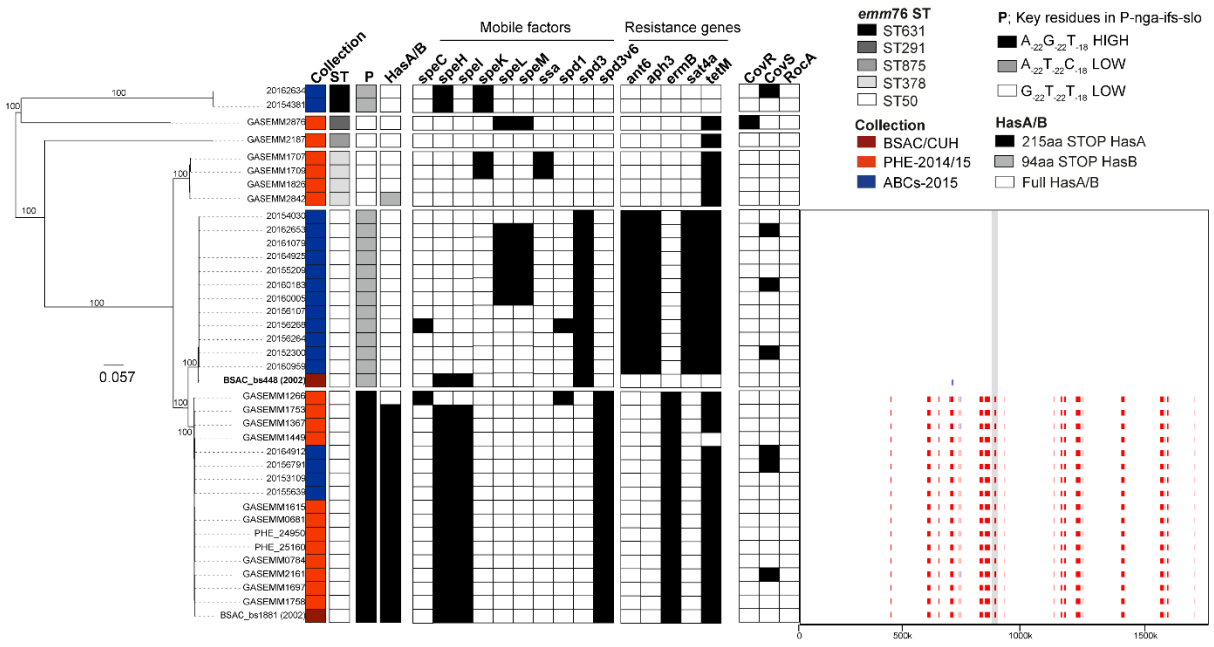
Collection
ST
P
HasA/B
Mobile factors
Resistance genes
speC
speH
speI
speK
speL
speM
ssa
spd1
spd3
spd3v6
ant6
aph3
ermB
sat4a
tetM
CovR
CovS
RocA
emm76 ST
ST631
ST291
ST875
ST378
ST50
Collection
BSAC/CUH
PHE-2014/15
ABCs-2015
P; Key residues in P-nga-ifs-slo
A-22G-22T-18 HIGH
A-22T-22C-18 LOW
G-22T-22T-18 LOW
HasA/B
215aa STOP HasA
94aa STOP HasB
Full HasA/B
0.057
0
500k
1000k
1500k

Figure S4

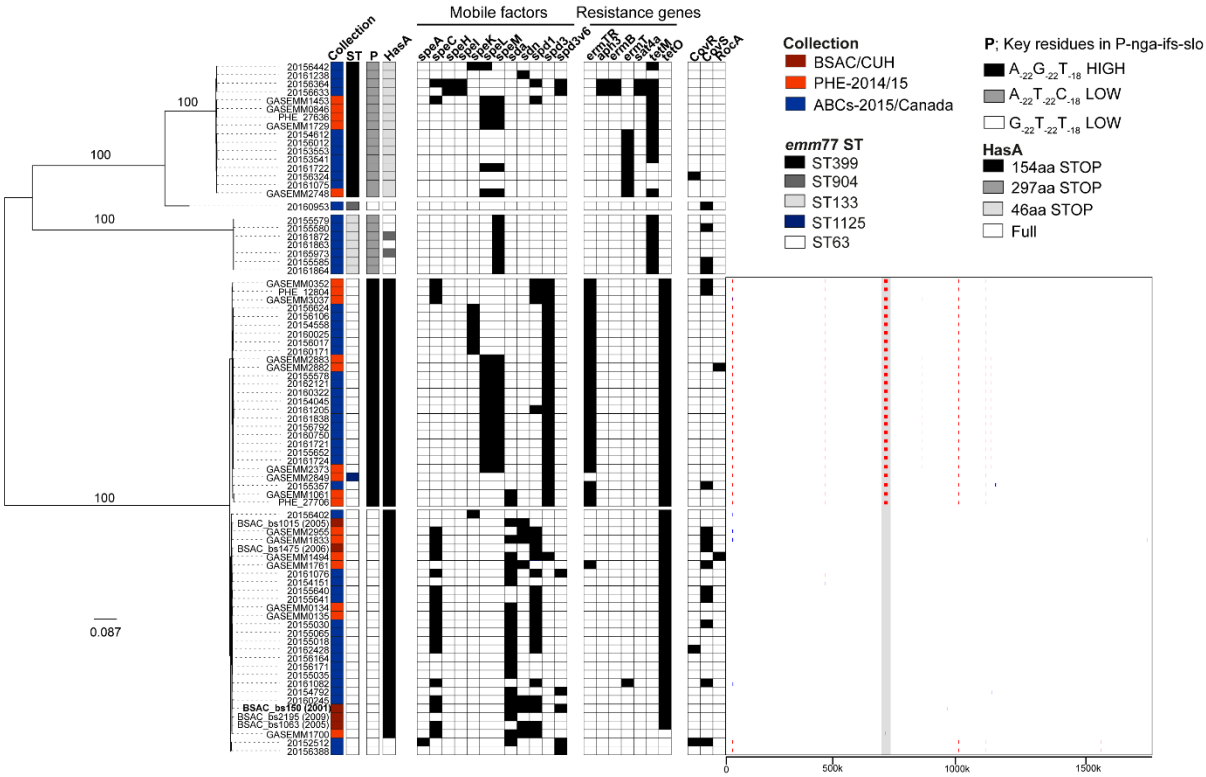
Mobile factors
Resistance genes
Collection
ST
P
HasA
speA
speC
speH
speI
speK
speL
speM
speQ
ssa
ssd1
ssd3
ssd3v6
ermTR
ermB
ermT
emmA
tetM
tetO
CovR
CiaR
RocA
100
100
100
100
0.087
Collection
BSAC/CUH
PHE-2014/15
ABCs-2015/Canada
emm77 ST
ST399
ST904
ST133
ST1125
ST63
P; Key residues in P-nga-ifs-slo
A-22G-22T-18 HIGH
A-22T-22C-18 LOW
G-22T-22T-18 LOW
HasA
154aa STOP
297aa STOP
46aa STOP
Full
0
500k
1000k
1500k

Figure S5

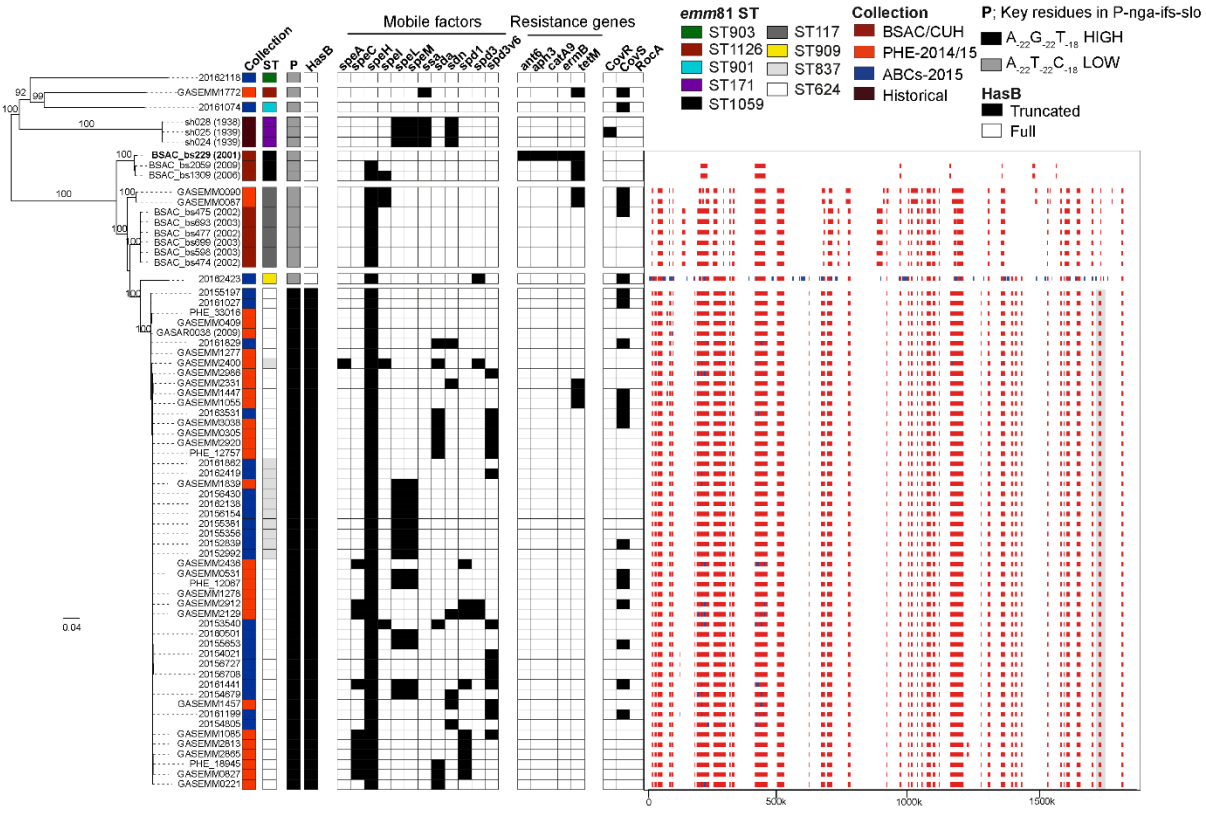
Collection
ST
P
HasB
Mobile factors
Resistance genes
speA
speC
speH
speI
speJ
speM
ssa
sph
spd1
spd3
spd3v6
ant6
aph3
catA9
ermB
tetM
CovR
CovS
RocA
emm81 ST
ST903
ST1126
ST901
ST171
ST1059
ST117
ST909
ST837
ST624
Collection
BSAC/CUH
PHE-2014/15
ABCs-2015
Historical
P; Key residues in P-nga-ifs-slo
A-22G-22T-18 HIGH
A-22T-22C-18 LOW
HasB
Truncated
Full
0.04
0
500k
1000k
1500k

Figure S6

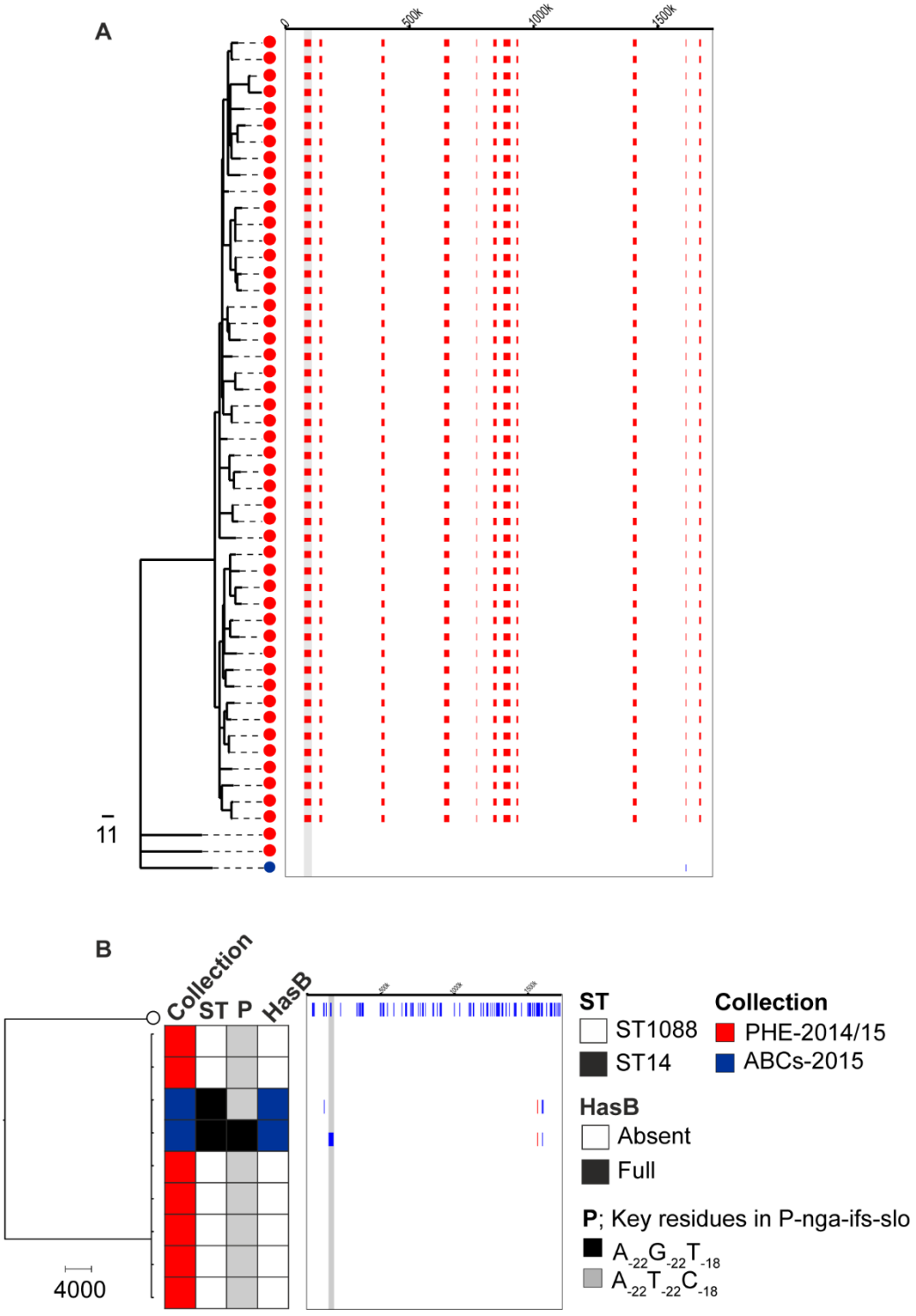
A
0
500k
1000k
1500k
11
B
Collection
ST
P
HasB
4000
ST
ST1088
ST14
Collection
PHE-2014/15
ABCs-2015
HasB
Absent
Full
P; Key residues in P-nga-ifs-slo
A-22G-22T-18
A-22T-22C-18